coatings

MDPI

Review

Perovskite Solar Cells: A Review of the Recent Advances

Priyanka Roy [1], Aritra Ghosh [2,*], Fraser Barclay [2], Ayush Khare [1] and Erdem Cuce [3,4]

[1] Thin Film Research Laboratory, Department of Physics, National Institute of Technology, G E Road, Raipur 492010, India; priyankaroy.gecraipur@gmail.com (P.R.); akhare.phy@nitrr.ac.in (A.K.)
[2] College of Engineering, Mathematics and Physical Sciences, University of Exeter, Penryn, Cornwall, Exeter TR11 2EL, UK; fb442@exeter.ac.uk
[3] Low/Zero Carbon Energy Technologies Laboratory, Faculty of Engineering and Architecture, Zihni Derin Campus, Recep Tayyip Erdogan University, Rize 53100, Turkey; erdem.cuce@erdogan.edu.tr
[4] Department of Mechanical Engineering, Faculty of Engineering and Architecture, Zihni Derin Campus, Recep Tayyip Erdogan University, Rize 53100, Turkey
* Correspondence: a.ghosh@exeter.ac.uk

Abstract: Perovskite solar cells (PSC) have been identified as a game-changer in the world of photovoltaics. This is owing to their rapid development in performance efficiency, increasing from 3.5% to 25.8% in a decade. Further advantages of PSCs include low fabrication costs and high tunability compared to conventional silicon-based solar cells. This paper reviews existing literature to discuss the structural and fundamental features of PSCs that have resulted in significant performance gains. Key electronic and optical properties include high electron mobility (800 cm^2/Vs), long diffusion wavelength (>1 μm), and high absorption coefficient (10^5 cm^{-1}). Synthesis methods of PSCs are considered, with solution-based manufacturing being the most cost-effective and common industrial method. Furthermore, this review identifies the issues impeding PSCs from large-scale commercialisation and the actions needed to resolve them. The main issue is stability as PSCs are particularly vulnerable to moisture, caused by the inherently weak bonds in the perovskite structure. Scalability of manufacturing is also a big issue as the spin-coating technique used for most laboratory-scale tests is not appropriate for large-scale production. This highlights the need for a transition to manufacturing techniques that are compatible with roll-to-roll processing to achieve high throughput. Finally, this review discusses future innovations, with the development of more environmentally friendly lead-free PSCs and high-efficiency multi-junction cells. Overall, this review provides a critical evaluation of the advances, opportunities and challenges of PSCs.

Keywords: perovskite solar cells; film fabrication; commercialization; issues; structure

Citation: Roy, P.; Ghosh, A.; Barclay, F.; Khare, A.; Cuce, E. Perovskite Solar Cells: A Review of the Recent Advances. *Coatings* **2022**, *12*, 1089. https://doi.org/10.3390/coatings12081089

Academic Editor: Cristian Vacacela Gomez

Received: 1 June 2022
Accepted: 29 July 2022
Published: 31 July 2022

1. Introduction

The ability to generate electricity from renewable energy sources is of great importance in the fight against climate change. The solar radiation incident on the Earth's surface is often regarded as the most abundant and safe energy source [1], because the sun provides the Earth's surface with four million exajoules of solar radiation annually [2]. In fact, one hour of sunlight on Earth provides more energy than what is used in one year, highlighting its importance [3]. The demand for clean energy has grown exponentially over the last decade, particularly in the area of solar photovoltaics (PV). This dramatic growth is shown by an increasing quantity of solar PV installed each year: for the very first time over 100 GW of solar PV was installed globally in the year 2018 [4], and is predicted to reach over 200 GW of newly installed capacity in the year 2022 [5]. Overall, solar PV capacity has now reached a total of 709 GW, representing 24.3% of overall global capacity [6]. The success of solar PV can be attributed to its practicality, low maintenance, and long lifetime [7]. Solar PV can also be installed and implemented in urban environments, unlike other renewable energy sources. This can be in the form of building applied photovoltaic (BAPV) and building

integrated photovoltaic (BIPV) [8,9]. This has led to a huge research effort to improve the efficiency of solar cells to extract as much energy as possible from solar irradiance.

The United Nations sustainable development (UN SDG) goal provides a blueprint to attain a better and sustainable future by 2030. This focuses upon several crucial aspects vital for humanity, among which increment in global percent of energy generation using renewables is one of the agendas. It is aimed to double the global rate of improvement in energy efficiency by 2030. The PV technology is the most efficient renewable energy capacity to meet future energy demands and has dragged the attention of researchers worldwide. Currently, silicon PV technology dominates the market. However, silicon PV technology alone cannot meet the energy demands in the future, and this has urged researchers worldwide to find an alternative and efficient PV technology, dragging the interest of researchers toward PSCs [10].

This inexhaustible resource can be converted into electricity via the photovoltaic effect using a semiconductor material [11]. The general working principle involves electromagnetic radiation from the sun, promoting an electron from the valence band to the conduction band. The energy difference between the valance band and conduction band is known as the bandgap and is a characteristic property of the semiconductor material. This creates electron-hole pairs and if these excited electrons are fed through an external circuit back to the valence band, an electrical current is created [12].

However, there is an upper limit to the power conversion efficiency (PCE) of a single junction solar cell, known as the Shockley–Queisser limit [13]. S. Rühle used this theory to calculate an up-to-date PCE for the global standard spectrum AM 1.5G [14]. The resulting PCE was 33.16% corresponding to a bandgap of 1.34 eV. There has been a lot of research into maximizing the PCE of the active materials used in photovoltaics.

The PV technology is progressing through generations of the cell, namely the first, second and third generations of a cell. The first generation of cells is basically wafer-based cells with thickness ranging from a few 100's of μm. First-generation solar cells are produced on silicon wafers. These solar cells dominate the market, having a global share of 90% [15]. There are two main types of silicon-based cells: mono-crystalline and polycrystalline. Monocrystalline solar cells are manufactured from single-crystal silicon that is obtained through the Czochralski process [16], which is energy-intensive and expensive. Monocrystalline solar cells are a mature technology and have achieved a PCE of 26.6% [17]. Polycrystalline solar cells are composed of a number of different silicon crystals. The manufacturing and processing costs are lower than for monocrystalline cells, but polycrystalline cells are less efficient.

The wafers of monocrystalline and multicrystalline silicon cells are continuing to dominate the industry. However, the production of ultra-pure semiconducting wafers is expensive in both finance and energy. The second-generation cells are based upon amorphous and polycrystalline semiconducting material deposited over the substrate. These cells are available at a low cost per unit of delivered energy as compared to the first generation of cells. However, many issues such as environmental, production process, material and scientific factors have hampered the market acceptance of the cell. The production share of the thin film cells is declining whereas the first generation of cells owing to their mature production technology is being produced cheaply in comparison to the second-generation cell [18]. Second-generation solar cells are also known as 'thin-film'; common examples include cadmium telluride (CdTe), copper indium gallium diselenide (CIGS) and gallium arsenide (GaAs). Thin-film cells are more economically viable as less material is required. These cells generally have a thickness of around 1 μm compared to around 350 μm for silicon wafers meaning they can even be utilized on curved surfaces [19,20]. The highest efficiency recorded in this group of materials is by GaAs, reaching a PCE of 29.1% [21]. Other notable mentions with high efficiencies are CdTe and CIGS achieving 22.1% and 23.35%, respectively [22,23]. However, each of the materials mentioned shows disadvantages in stopping commercialization on a major scale. GaAs have a difficult and expensive manufacturing process making them only useful in high-efficiency applications [24]. CIGS

and CdTe are restricted by their required materials, using rare elements such as indium and tellurium along with toxic materials such as cadmium [25]. The thin film technology is still under way in terms of attaining high performance at a low cost. Therefore, it can be said that Si technology has successfully dominated thin film technology. Thin film solar cells have the advantage of being rollable and foldable leading to minimal risk of falling. They are lightweight cells with the ability to generate electricity under both low- and high-intensity of incident illumination. Some of the established thin film solar cells are gallium arsenide (GaAs), cadmium telluride (CdTe) and copper indium gallium selenide (CIGs). Among all the existing thin film photovoltaic technologies, cadmium telluride (CdTe) occupies more than 95% of the thin film solar cell market because of its mature technology and minimum cost. Thin film solar cells are more widely used in wearable devices and building integrated photovoltaics (BIPVs) than in PV plants [26].

Third-generation solar cells are still under development but have achieved promising results and are improving rapidly. These materials benefit from low-energy manufacturing processes and low-cost materials, making them an attractive proposition. There are various types of solar cells being tested such as dye-sensitized, quantum dot, and perovskite solar cells. From the third-generation solar cells, perovskite solar cells are the most promising. Over the last decade, solar devices based on perovskite have seen the PCE jump from 3.5% obtained by Kojima et al. [27], to 25.8% by [28,29]. The third generation of cells is referred to as 'emerging technologies'. This generation includes organic photovoltaic technology (OPVs), copper zinc tin sulfide (CZTs), quantum dot cells, dye-sensitized solar cells (DSSC), and perovskite solar cells. This generation of cell has exhibited the potential of low cost and easy production without compromising the performance of the cell [30]. In this work, we focus on perovskite solar cells (PSCs). The performance and stability of OPVs are limited, although researchers are working towards the improvement of performance and stability. Ahsan Saeed et al. [31] replaced the conventional fullerene derivative-based ETL (PCBM) due to its photo-instability and inefficient light absorption ability. They used (poly[(2,6-(4,8-bis(5-(2-ethylhexyl)thiophen-2-yl)-benzo [1,2-b:4,5-b']dithiophene))-alt-(5,5-(1′,3′-di-2-thienyl5′,7′-bis(2-ethylhexyl)benzo [1′,2′-c:4′,5′-c']dithiophene-4,8-dionz) and a modified ITIC-based NFA (3,9-bis(2-methylene-(3-(1,1-dicyanomethylene)-indanone))-5,5,11,11-tetrakis (4-hexylmeta-phenyl)-dithieno [2,3-2′,3′-d']-s indaceno [1,2b:5,6b] dithiopheneethylexyloxy) (m-ITIC-O-EH) a wide bandgap donor with alkoxy side chains. Owing to better absorption properties of m-ITIC-O-EH, performance three times higher than that of PCBM-based OPV is attained. Dye-sensitized solar cells are also used for indoor applications [32]. The popularity of DSSCs owes to their easy production process and low cost. Natural dyes are also used as sensitizers which eliminate the use of a high-cost synthesis process enabling a simple extraction process [33]. Organic photovoltaics (OPVs) are widely used for indoor applications and self-powered electronic devices for internet-of-things (IoT) applications [34].

The PSCs have the capability to attain high efficiency at a low cost as compared to other established cells. PSCs seem to be the potential candidate for attaining high efficiency at low material and low processing costs. The highest advantage that perovskite material holds over conventional PV is its ability to react towards a different range of wavelengths of light, such that maximum incident radiation is converted to electricity. The fact that it can be fabricated over a flexible substrate enables its application in different ways. The PSCs offer the advantage of being lightweight, comprising tailored form factor, easy producible and scalability and many more. Despite being a potential candidate, it is still at the beginning stage of commercialization as compared to other solar technology. The efficient PSCs still contain Au as an electrode which increases the cost of the device. Exploring the low-cost electrode can overcome this shortcoming. Most of the leading PSCs are Pb based, making them toxic in nature. Studies are being conducted to replace the toxic Pb, but still, none of the Pb-free PSCs has defeated the highest performance attained by Pb-based PSCs. The scientific community is actively searching for Pb alternatives to address the issue of toxicity. Metals such as Tin (Sn), germanium (Ge), rubidium (Rb),

bismuth (Bi), and antimony (Sb) have all been reported to generate non-toxic or less-toxic metal halide perovskite materials, and their use in PSCs has been proven to be effective [35]. Among all the alternatives, Sn has exhibited the best performance. The Sn-based PSCs were lagging in performance as compared to Pb-based PSCs, due to poor stability of the formed perovskite and improper energy level mismatch between the charge transport layer and perovskite. These issues were combated by Nishimura et al. [36]. They controlled the A-site cation of the perovskite to regulate the tolerance factor value by one. They partially substituted formamidinium cation (FA) with ethylammonium cation (EA) which not only helped attain the highest PCE of 13% to date but also enhanced the stability of the device. Currently, the most efficient PSCs have attained the best performance by the modification in the charge transport layer and at the interfaces. Min et al. [37] placed an interface layer (IL) between ETL and absorber layer. A defect-free connection layer is added. The presence of the IL eliminated the need for passivation. The IL has inherent properties which improve charge carrier transport and extraction from the perovskite layer. This modification also reduced interfacial defects. This work provides us with the guidelines to design minimum defect interfaces between ETL and the perovskite layer. With this modification, a high PCE of 25.5% is obtained with 90% of PCE retained after 500 h of operation. Researchers from the Swiss Federal Institute of Technology Lausanne (EPFL) have enhanced the scalability by replacing ETL with quantum dots. Further high PCE of 25.7% is obtained with high operational stability. The ETL material is replaced by the quantum dots of Tin (IV) oxide. The ETL fabrication had a negative impact on the scalability of the device. Until now, the most widely used ETL material is mesoporous-TiO_2. This widely used ETL has the drawback of low electron mobility and also is susceptible to negative photocatalytic events under ultraviolet illumination. The usage of QDs as ETL has enhanced the light trapping efficiency and reduced the charge carrier recombination [38]. Azam et al. [39] demonstrated the role of interfaces across the perovskite absorber layer and perovskite layer defect passivation on the device performance and stability. They used organic chlorinated salt (benzyl triethylammonium chloride) across the interfaces. This led to better film morphology with proper band alignment across charge transport layers, which rendered considerable improvement in device performance and stability.

2. Methods

This review focuses on perovskite solar cells, hailed as the most promising new-generation solar cells. The structure of perovskite is investigated, identifying the key features responsible for effective use in solar cells. The key advances along with the processing, issues, and the future of perovskite solar cell technologies are outlined.

Academic peer-reviewed journal articles were used as the primary literature source for the review. Appropriate articles were found through Google Scholar and ScienceDirect search engines [40,41]. Searching keywords such as 'perovskite' often afforded a large number of publications. The search was then refined to only include papers published in recent years in order to find the latest advances in technology. Following this, if more specificity was needed the advanced search functions were utilized so that the keywords must appear in the title of the paper. This method was an effective way of finding appropriate papers for this review.

3. Results

3.1. Structure

The nomenclature for any material that has the same crystal structure as calcium titanate ($CaTiO_3$) is 'perovskite' [42]. Perovskite consists of a crystalline structure with composition ABX_3, in general A and B are cations and X is oxygen or a halogen anion. The crystal structure of perovskite is pictured in Figure 1.

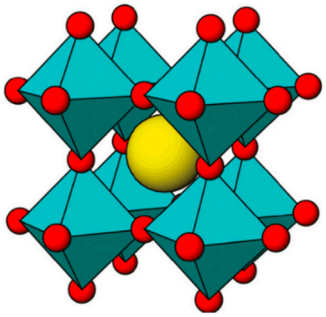

Figure 1. Crystal structure of perovskite: A-cation (yellow), B-cation (blue octahedra), X-anion (red). Reprinted with permission from Ref [43]. Copyright (2020) ACS publications.

Each B-cation is surrounded by six anions, creating $[BX_6]^{4-}$ octahedra. These are connected via corner-sharing and effectively form the ReO_3 structure [44]. The difference being the cuboctahedral site is occupied by the A-cation in perovskite structures [45]. One of the major benefits of the perovskite structure is the ability to integrate elements with different valences into the structure. For example, if X is an oxygen anion (O^{2-}), cations A and B would be divalent and trivalent, respectively. However, if X is a halogen anion (Cl^-, Br^-, I^-), then the cations A and B would be monovalent and divalent [46]. This provides a great opportunity to easily modify the properties such as the bandgap of the material. Figure 2a exhibits the evolution of efficiency with progressive years of PSCs, Figure 2b exhibits the various cations and anions that can be used in perovskite materials with middle circle material depicting the widely used composition.

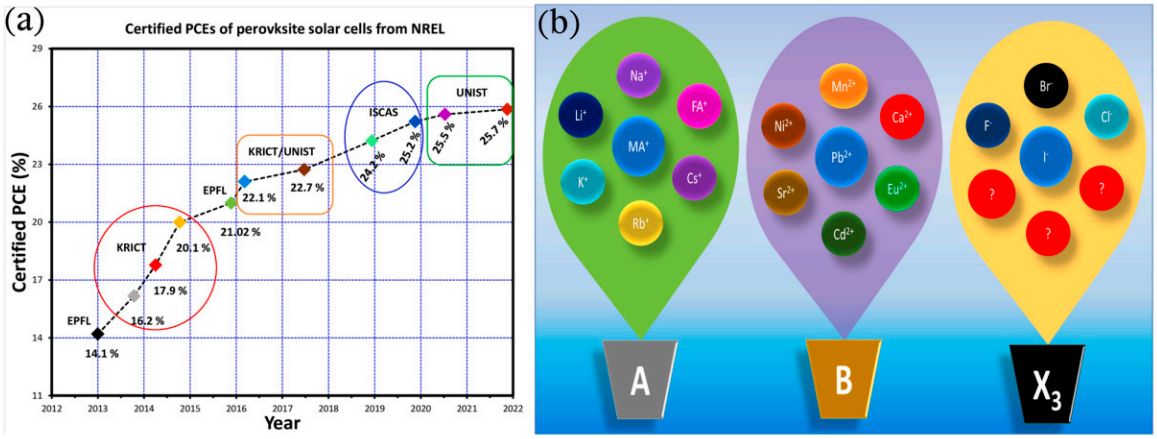

Figure 2. (**a**) Certified PCEs of perovskite solar cells achieved by different groups, data collected from NREL website on 30 March 2022. (**b**) Schematic diagram of ABX3 perovskite with possible A-and B-site (cations) and X-site (anions) dopant passivators (middle circles in blue color indicate the widely used composition of ABX3 PSCs). Reproduced with permission from ref [47].

The tuning of perovskite structures will be discussed in more detail in a later section of this review. The ion sizes used in perovskites are an important factor dictating the final structure and stability [48]. The goldsmith tolerance factor is the most commonly used and successful ratio [49].

The Goldsmith tolerance factor:

$$t = \frac{r_A + r_X}{\sqrt{2}(r_B + r_X)} \quad (1)$$

Here r_A is the radius of cation A, r_B is the radius of cation B and r_X is the radius of anion. The tolerance factor is effectively a measure of how well the A-cation fits into the framework. The limits for perovskite structure formation are: $0.8 \leq t \leq 1$, with

the upper limit 1 describing the perfect fit [50]. For tolerance factors approaching the lower limit of 0.8, the structure will be distorted due to the tilting of the BX_6 octahedra. Tolerance factors above 1 indicate that the cation is too large to fit into the site, stopping perovskite formation. The tolerance factor is an important consideration when designing new materials for perovskite solar cells. Deviation from the specified range may result in alternative structures that do not have the same properties as perovskites.

3.2. Device Structure

The device structure of PSCs basically contains an absorber layer, an electron transport layer (ETL), a hole transport layer (HTL), a transparent conductive oxide (anode) and a metal contact (cathode). The incident light enters through the transparent conductive oxide (FTO or ITO) towards the perovskite absorber layer. The schematic of the device structure in both nip structure and pin structure is shown in Figure 3a,b, respectively. The absorber layer upon absorption of the incident radiation creates electron and hole pairs. These generated electrons and holes are transported via ETL and HTL, respectively, towards the external circuit with the help of charge collecting contacts. The material to be used in ETL and HTL must have the required band alignment with respect to the absorber layer to ensure proper carrier collection [51,52]. In order to obtain the best possible performance from the PSC, all three layers of materials must be wisely selected and fabricated. Roy et al. [53], demonstrated the role of layer thickness and carrier concentration requirement for all three layers. They revealed that the optimum transport layer (both ETL and HTL) thickness must be as minimum as possible until it ensures proper film coverage across the perovskite layer. The optimum absorber layer thickness is equivalent to the carrier diffusion length of the perovskite. Roy et al. [54] further explained the role and requirement of the energy level tuning across the perovskite/HTL and ETL/perovskite interfaces.

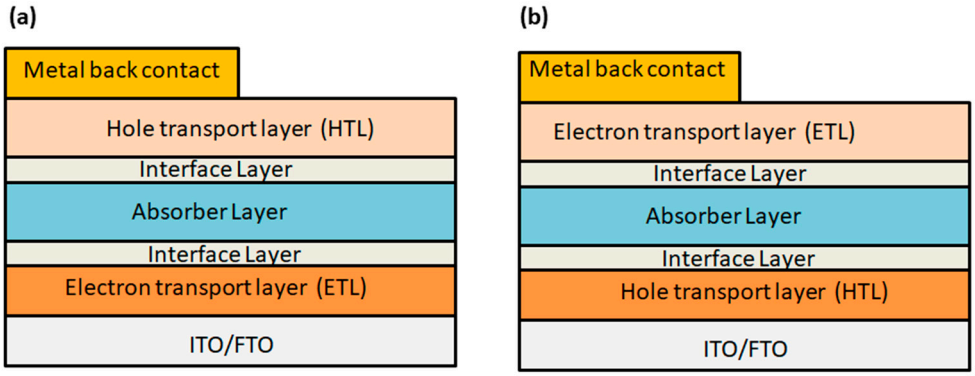

Figure 3. Demonstration of device structure of PSC: (**a**) n-i-p structure, (**b**) p-i-n structure.

The transport layers can employ both organic and inorganic materials. The organic HTLs require extremely high purity and cost. The widely used HTL Spiro-OMeTAD costs are ten times higher than Platinum and Gold. Moreover, certain studies suggest that the organic HTLs actively participate in the process of degradation, which contributes to the poor stability of PSCs. The future development of PSCs requires a wise selection of the HTL. The inorganic HTLs seem to be a potential alternative. The inorganic P-type semiconductor such as nanotubes, nanocrystal, quantum dots and nano powder contributes towards the increment of the performance of the PSCs. The inorganic HTLs are low cost and easy to synthesise with better stability. An appropriate energy level matching is required with perovskite before selecting any particular material. The key points to be considered while selecting an appropriate material for HTL are: (i) the highest occupied molecular orbital (HOMO) energy level in inorganic p-type semiconductor should be at a proper position with respect to the valance band of the perovskite layer to enable proper charge transport and hole collection for better obtaining better current density; and (ii) there must be less special contact between perovskite and HTL to reduce the carrier recombination

as it reduces the open circuit voltage (V_{oc}) of the cell. Various materials that can be used as inorganic HTLs are: graphene oxide (GO), carbon (C), Copper thiocyanate (CuSCN), Copper Zinc Tin Sulfide ($CuZnSnS_2$), Copper indium disulfide ($CuInS_2$), Copper iodide (CuI), Cuprous oxide (Cu_2O), Cupric oxide (CuO), Nickel oxide (NiO) and a few more [55]. Figure 4 exhibits the efficiency tree of PSC using different materials at HTLs. The ETL layer also contributes significantly to the PCE and device stability. The most widely used ETL is Titanium dioxide (TiO_2), due to its superior stability. However, the fact that it requires high annealing temperature and assists the process of ion immigration leading degradation of the cell urges to find an alternative. Various ETL materials are ZnO, CdS, PCBM, SnO_2 etc. Currently, the most popular ETL material is SnO_2 due to its wide bandgap 3.6–4.1 eV with deeper conduction band (CB) than TiO_2. It is the most potential ETL due to: (i) higher mobility 240 cm^2/V, (ii) deeper CB leading to enhanced collection and transportation of charge carrier, (iii) wider bandgap, (iv) low temperature fabrication and (v) high optical transmittance and conductivity [56].

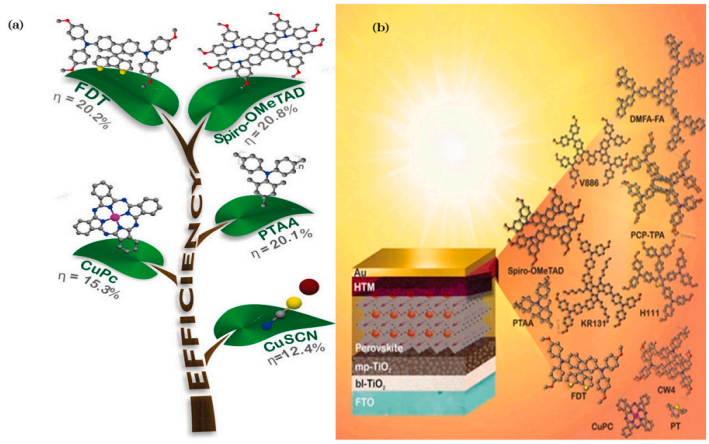

Figure 4. (**a**) The efficiency improvement tree of perovskite solar cell using different hole transporting layers. (**b**) Device architecture and molecular structure of commonly used hole transporting materials. Reproduced with permission from ref [47].

A transparent conductive electrode (TCE) is the key component for the working of a solar cell as it not only passes the incident radiation towards the absorber layer but also it extracts the photo-generated charge carriers towards the external circuit. Proper transparency and conductivity are the key features of TCEs [57]. There must be a proper balance between transparency and conductivity for an efficient TCE. The selection of an appropriate TCE is important and is determined by a parameter called Figure of Merit (FOM). A novel FOM signifies Figure 4a as the proportionality of output power from PV devices, while Figure 4b provides guidance for the development of advanced TCEs. On the basis of exact FOM, the transition sheet resistance is defined which separates two operating regimes of TCEs (transmittance and conductance) [58,59].

3.3. Fundamental Features

In order to design perovskite solar cells with the highest PCE possible, the fundamental properties of the material must be understood. This includes the optical and electronic properties of the light absorber, along with how the photogenerated charges are collected [60].

Perovskite materials contain unique properties that make them effective PV devices. The high efficiency is credited to the high electron mobility (800 cm^2/Vs) along with a long diffusion wavelength (>1 μm) [61,62]. They also have a high absorption coefficient (10^5 cm^{-1}), caused by s-p antibonding coupling [63]. Another beneficial property of perovskite materials is a low exciton binding energy, measured to be less than 10 meV. This allows the excited carriers to migrate as free carriers. These characteristic properties and

their associated values are summarised in Table 1. The combination of the beneficial features described above makes perovskite an effective material for photovoltaic use.

Table 1. Summarising the optical and electronic properties of perovskite materials. Reprinted with permission from Roy et al. [64].

Properties	Value Rangege
Bandgap	1.5–2.5 eV
Absorption coefficient	10^5 cm^{-1}
Exciton binding energy	Less than 10 meV
Crystallization energy barrier	56.6–97.3 kJ mol^{-1}
PL quantum efficiency	70%
Charge carrier lifetime	Greater than 300 nm
Relative permittivity	3
Carrier mobility	800 cm^2/Vs
Exciton	Wannier type exciton
Trap-state density	10^{10} cm^3 (single crystals), 10^{15}–10^{17} cm^3 (polycrystalline)

Table 1 shows that the bandgap for perovskite materials can have a large range, which results from their easy tunability. The perovskite structure allows a large amount of changeability. The perovskite material $CH_3NH_3PbI_3$ is the most commonly used and the amine, metal and halide can all be altered to form different perovskite materials. Modification of the amine from methylammonium ($CH_3NH_3^+$) to alternative amines has been investigated. Using an extended alkyl chain such as ethyl ammonium ($CH_3CH_2NH_3^+$) has been successfully synthesized and showed a larger bandgap and lower PCE of only 2.4% [65]. An alternative amine substitution is to use the formamidinium cation ($NH_2CH{=}NH_2^+$). This has shown very successful results with an experimentally determined bandgap as low as 1.47 eV; this is better than the 1.55 eV achieved by methyl ammonium-based perovskites and closer to the Shockley–Queisser limit [66]. This cell also achieved an impressive PCE of 14.2% [67]. Additional work has been completed to create a mixed cation perovskite using the formamidinium and methylammonium cations. This approach resulted in enhanced stability and an improved PCE of over 18% [68,69]. Table 2 encloses various PSC configurations along with their attained performance parameters.

Additionally, the iodide anion can be substituted for other halides (Cl^-, Br^-) in order to tune the bandgap. The general trend is that the bandgap decreases upon increasing halide size, making iodide the closest to the ideal limit [70]. However, the opposite trend is observed for stability with methylammonium lead iodide having the lowest reaction enthalpy compared to equivalent chloride and bromide-based-perovskites, making it the most unstable [71]. In order to achieve both stability and performance the mixed halide perovskite $CH_3NH_3PbI_{3-x}Br_x$ was tested; it had a tunable bandgap between 1.6–2.3 eV depending on the bromide composition [72]. This can be an extremely useful feature that can be used in tandem solar cells, discussed later in this review. Several different materials (such as Sn, Ge, Bi, Sb, and a few more) are used in place of lead (Pb) metal cation to tackle the issue of toxicity. However, the performance attained by lead-free perovskite-based PSCs still lags behind the lead-based PSCs [73]. Attempts to replace the lead metal cation still require more attention from the research community due to poor efficiencies [74].

Table 2. Performance attained by various configurations of PSCs with progressive years.

PCE (%)	V_{oc}(v)	J_{sc}(mA/cm^2)	FF	Device Configuration	Year	Reference
2.02	0.24	22.7	0.37	FTO/Compact TiO_2/Mesoporous TiO_2/Perovskite/m-MTDATA/Au	2014	[75]
4.63	0.57	13.2	0.61	FTO/TiO_2/Dye/Cs_2SnI_6 + Z_{907}/Pt	2014	[76]
6.32	0.63	14.7	0.68	FTO/TiO_2/Dye/Cs_2SnI_6 + N_{719}/Pt		
6.94	0.62	16.9	0.66	FTO/TiO_2/Dye/Cs_2SnI_6 + multiple/Pt		
6.4	0.88	16.8	0.42	TiO_2/m-TiO_2/$MASnI_3$/SpiroOMeTAD + LiTFSI + tBP/Au	2014	[77]
6.7	0.6	17.53	0.65	ITO/NiO_x/$FASnI_3$/PCBM/Ag	2018	[78]
7.11	0.63	18.61	0.606	FTO/PCBM/$CsSn_{0.5}Ge_{0.5}I_3$/Spiro-OMeTAD/Au	2019	[79]
7.37	0.73	15.8	0.64	Au/TiO_2/m-TiO_2/$MASn_{0.25}Pb0._{75}$/Spiro-OMeTAD/Au	2014	[80]
7.66	0.97	11.1	7.66	ITO/ZnO/$MASnI_3$/spiro-OMeTAD/Au	2015	[81]
9	0.52	24.1	0.71	ITO/PEDOT:PSS/$FASnI_3$/C_{60}BCP/Ag	2017	[82]
9.2	0.61	21.2	0.72	ITO/PEDOT:PSS/$GA_xFA_{0.98-x}SnI_3$–1% $EDAI_2$/C_{60} (20 nm)/BCP/Ag	2018	[83]
9.8	0.76	19.1	0.66	ITO/PEDOT:PSS/$MAPb_{0.85}Sn_{0.15}I_{3-y}Cl_y$/$PC_{61}$BM/Ag	2014	[84]
10.2	0.72	19.2	0.73	FTO/TiO_2/N719 Dye/Perovskite/ZnO	2012	[85]
12.1	0.78	20.65	0.75	ITO/PEDOT: PSS/$MASn_{0.6}Pb_{0.4}I_{3-x}Br_x$/PCBM/Ag	2017	[86]
13.24	0.84	20.32	0.78	FTO/PEDOT PSS/$EA_{0.98}EDA_{0.01}SnI_3$/C_{60}BCP/Au	2020	[87]
14.06	0.79	22.8	0.78	ITO/PEDOTPSS/$MA_{0.5}FA_{0.5}Pb_{0.75}Sn_{0.25}I_3$/$PC_{61}$ BM/C_{60} /Ag	2016	[88]
10.2	0.7	21.9	0.66	ITO/PEDOT:PSS/FASn0.5Pb0.5I3 /C60 BCP/Ag	2016	[89]
14.1	0.74	26.1	0.71	ITO/PEDOT:PSS/C60 BCP/Ag		
15.08	0.79	26.86	0.70	ITO/PEDOT:PSS/$(CH_3NH_3)_{0.4}[HC(NH_2)_2]_{0.6}Sn_{0.6}Pb_{0.4}I_3$/$C_{60}$/BCP/Ag	2016	[90]
17.55	1.03	21.9	0.78	ITO/PEDOT:PSS/$MAPb_{0.85}In_{0.15}I_3Cl_{0.15}$/$PC_{61}$ BM/Bphen/Ag	2016	[91]
18	1.02	22.4	0.78	FTO/SnO_2/$Cs_{0.16}FA_{0.84}Pb(I_{0.88}Br_{0.12})_3$/Spiro-OMeTAD/Au		[92]
19.1	1.01	22.4	0.78	FTO/Poly-TPD/0.15 mol% Al_3+-doped CH3NH3PbI3/PCBM/BCP/Ag	2016	[93]
22.3	1.71	24.1	0.81	ITO/PTAA/$Cs_{0.05}(FA_{0.92}MA_{0.08})_{0.95}Pb(I_{0.92}Br_{0.08})_3$/$C_{60}$/BCP/Cu	2020	[94]
23	1.16	24	0.82	Glass/ITO/PTAA/$(Cs_{0.05}(FA_5/MAI)_{0.95}Pb(I_{0.9}Br_{0.1})_3)$/PCBM/BCP/Ag	2021	[95]
23.7	1.16	24.16	0.84	Glass/ITO/PTAA/PEAI/$(Cs_{0.05}(FA_5/MAI)_{0.95}Pb(I_{0.9}Br_{0.1})_3)$/PEAI/PCBM/BCP/Ag	2021	[96]
24.6	1.05	25.5	0.83	FTO/SnO_2/$(FAPbI3)_{0.95}(MAPbBr_3)_{0.05}$/P3HT/Au		[97]
24.8	1.16	26.35	0.8	FTO/c-TiO_2/m-TiO_2/$FAPbI_3$/Spiro-OMeTAD/Au	2020	[98]
25.4	1.19	25.09	0.84	FTO/SnO_2/$MAPbBr_3$/HTL/back contact	2021	[99]
25.5	1.18	25.74	0.83	FTO/SnO_2-Cl/$FAPbI_3$/Spiro-OMETAD/Au	2021	[37]

3.4. Perovskite Films Preparation

Perovskite solar cells use more abundant and cost-effective elements and have a simpler manufacturing process than silicon-based solar cells [100]. The manufacturing of silicon solar cells involves high temperatures in excess of 1000 °C in a highly evacuated chamber [101]. In contrast, perovskites can be manufactured using simple wet chemistry, with no requirement for an evacuated environment. The conditions and techniques used to prepare the perovskite film are crucial for crystallinity, controlling the performance of the cell. The factors that need to be strictly controlled have been identified as atmospheric conditions during film growth, reagent stoichiometry, a method to deposit perovskite on the substrate, annealing temperature/duration, and additives used. There are three main methods for preparing perovskite films: solution processing, vapor deposition and hybrid vapor-solution processing.

The most common and cost-effective method of synthesizing the perovskite film is solution processing. This can either be through a one-step method or a two-step sequential method. The one-step method involves the spin-coating of a pre-mixed solution that is typically prepared by blending CH_3NH_3X powder with PbX_2 in a 1:1 molar ratio. The two-step sequential method first spin-coats PbI_2 over a TiO_2 substrate before being dipped in a CH_3NH_3X solution [102]. This method allows perovskite to be more effectively implemented into the substrate's mesoporous layer. Although the two-step method has produced solar cells with higher PCEs to date, the one-step is preferred [103]. Figures 5 and 6 depict the schematic illustration of one-step and two-step solution processing techniques, respec-

tively. This method is less complex and allows superior control of the crystallinity and morphology. Therefore, this technique provides the potential to control the grain growth and hence achieve a much higher PCE in the future.

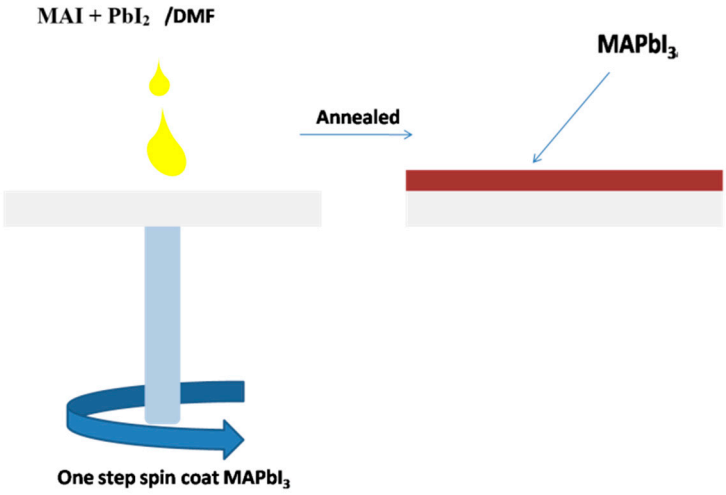

Figure 5. Schematic illustration of one-step solution processing method. Reprinted with permission from Ref [64]. Copyright (2020) Elsevier.

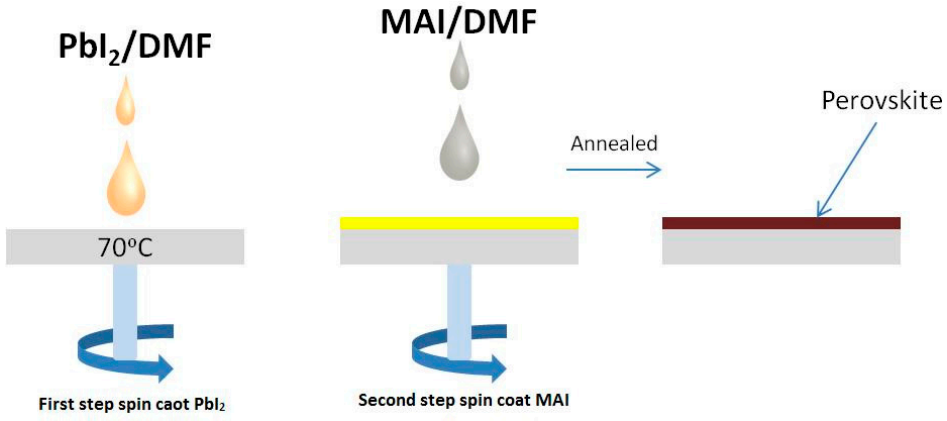

Figure 6. Schematic illustration of two-step solution processing method. Reprinted with permission from Ref [64]. Copyright (2020) Elsevier.

Vapour deposition produces planar perovskite solar cells by evaporating CH_3NH_3X and PbX_2 at the same time. Liu et al. co-evaporated CH_3NH_3I and $PbCl_2$ at 120 °C and 350 °C, respectively, in a glovebox under inert nitrogen gas [104]. The perovskite was deposited on a TiO_2 layered FTO glass before annealing produced the crystalline material. This technique produces high-quality uniform films, which reach high PCE's. However, this method requires high vacuum levels for thermal evaporation, and this can be expensive. This presents a big barrier and impedes mass production as it is not economically feasible [105]. Another notable mention is a hybrid method developed by Chen et al. called vapour assisted solution process [106]. This technique involves first depositing a thin PbI_2 film on the substrate before reacting with CH_3NH_3I vapor. This method produces excellent quality perovskite films in a more controllable process than solution processes, but once again requires expensive conditions. Smecca et al. developed a new film deposition technique, called low vacuum proximity space-effusion (LV-PSE). This is a two-step method capable of fabricating high-quality film at minimum cost and wastage. In this process, the conversion of PbI_2 film into $MAPbI_3$ film at a given temperature begins from the top surface by an adsorption–incorporation–migration mechanism, followed by the gradient of energetic MAI concentrations. Their work stated that with the use

of this new film fabrication technique, better efficiency along with reduced cost can be obtained. This method also addresses environmental concerns by reducing the usage of Pb content within the device [107]. Vesce et al. developed a blade-coating strategy at ambient air for fabricating stable triple cation (CsMAFA) PSCs. This is a two-step blade process using the green antisolvent quenching technique. This method is industry compatible and capable of producing efficient small area cells with high reproducibility [108]. Ming He et al. demonstrated a low-temperature solution processing-based inkjet printing technique for perovskite film fabrication. The cell fabricated using MASP (meniscus assisted solution printing) technique enabled attaining efficiency of 20% by controlling the orientation and crystal size of the perovskite molecules. This technique uses 300 µm apart two parallel plates to form a meniscus of ink (comprising perovskite precursor). This MASP technique generates perovskite of large crystal size typically of order 20–80 µm diameter. This technique offers the advantage of fabricating films with a denser and lower number of perovskite crystals. This leads to minimizing the gaps between the crystals which hinders the current flow and also reduces the electron-hole recombination traps, enhancing the charge carrier extraction from the cell [109]. Huang et al. produced a modified one-step solution processing technique that can produce stable PSCs at a large scale and overcome the issue of commercialization. Sulfolane is added as an additive in the precursor solution. It can be added to the liquid material that aids the perovskite crystal formation via a chemical reaction. The simple dipping method enabled the deposit of high-quality films with uniform coverage at two mini-modules. The efficiency attained by both the modules was 17.58% and 16.06%, respectively. The use of sulfolane enhances the processing window of the precursor solution from 9 to 90 s. This leads to the formation of a compact layer of high crystallinity over a large area [110]. Various modifications in the film deposition process have a substantial impact on the stability and the performance of the cell.

Various methods of production for large area perovskite are solution processing and vapor deposition based methods. The solution processing methods are vacuum flash-assisted solution process, blade coating, slot-die coating, spin coating, ink-jet printing and spray coating. The vapor deposition methods are chemical vapor deposition, vapor assisted solution process, flash evaporation, sequential evaporation, co-evaporation, and vapor thermal evaporation. Spray coating and blade coating processes were widely used initially and have not lost its charm. The inkjet printing and slot-die coating processes are widely used for the production of large area PSCs. The highest efficiency for large area PSCs is attained by slot-die coating process [111]. Conventional 156 mm × 156 mm Si bottom cell is 20–22% efficient. Upon using perovskites with Silicon in a tandem structure cell the efficiency reaches about 30% [112,113]. Ashouri et al. [114] fabricated a monolithic perovskite/silicon tandem cell with an efficiency of more than 29% with the help of enhanced hole extraction. They stabilized the perovskite with 1.68 eV bandgap enabling proper charge transfer. The formation of a self-assembled monolayer acted as an efficient hole selective contact which reduced the non-radiative recombination enhancing the efficiency.

4. Discussion

4.1. Issues

The biggest issue facing the commercialization of perovskite solar cells is a lack of stability. These problems arise from the chemical interactions within the perovskite structure. The interactions mostly consist of weak ionic bonds, e.g., the Pb-I bond has a bonding energy of 142 $kJmol^{-1}$ [115]. Other secondary interactions are hydrogen bonding and van der Waals forces, giving the material its soft nature [116]. Perovskite solar cells are inherently sensitive to heat, light, moisture, electric fields and oxygen that can all degrade the cell [117]. Particular sensitivity to water and moisture was highlighted by Niu et al., concluding that iodide perovskites have a negative standard Gibbs free energy with regards to moisture degradation [118]. These stability issues must be addressed in order for perovskite cells to have a long operational life and be commercialized. Further research must be conducted to determine the exact degradation mechanisms, allowing appropriate stabilisation and

encapsulation approaches to be developed. Figure 7 summarizes various strategies that can be adopted to improve the device stability along with overall device performance.

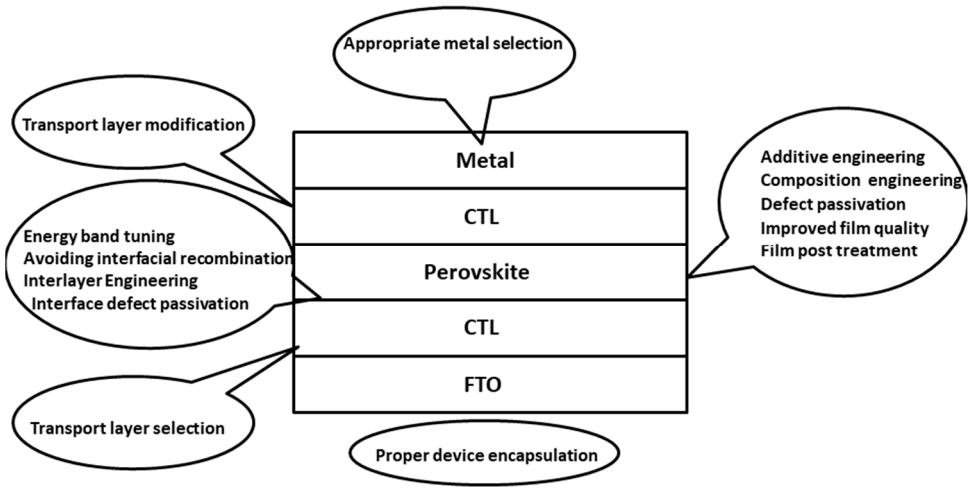

Figure 7. Various strategies to improve stability and avoid degradation in PSCs.

Composition engineering is an effective approach for the stability and performance enhancement of the PSCs [119]. In this strategy, the anion and/or cation of the perovskite material with crystal structure ABX_3 is substituted either partially or totally with a desirable material improving the optoelectronic property of the device. In the perovskite material $MAPbI_3$, the conduction band minima are directed by the p-orbital of Pb. The valance band maxima are directed by s and p orbital of Pb and p-orbital of I. The A-site of the perovskite structure does not contribute to the band edge but contributes to the deep energy level of the material. Studies suggest that on tuning A-site the optoelectronic properties of the material can be easily tuned [120]. These modifications also improve other factors, such as thermal stability. The substitution of FA in place of MA at A-site, leads to a stronger bond formation with PbX_6 octahedra due to the presence of a larger number of H-bonds. This not only modifies the optoelectronic property of the material but also enhances the thermal stability [121]. The substitution of an inorganic cation such as Cs in place of MA has proved to form stronger bonds as compared to H-bonds. Similarly, mixed halide perovskites have exhibited better stability and efficiency [122]. The partial substitution of X-site I by other halides is another strategy of composition engineering. The substitution of I by Br and Cl increases bandgap and reduces the device efficiency. Therefore, limited substitution has to be done such that efficiency is not much reduced and better stability is attained [123]. Apart from the basic components, the addition of certain materials as an additive has the capability to enhance the performance of the PSC. Several studies have been conducted and certain materials are proven beneficial for the PSCs. Additives can be classified into two categories: (i) additives with precursor of one-step method; (ii) additives with organic solvent at two-step solution method, and additives with antisolvents. This is a broad research field and several reviews based on it can be easily obtained from the literature [124]. The material used along with the quality of the charge transport layer (CTL) affects the performance of the PSCs. The material for the electron transport layer (ETL) must be selected such that the conduction band edge is either equal to or lower than the conduction band of perovskite material, such that the photogenerated electrons from the perovskite layer can be easily received. The valance band of the ETL must lie below the perovskite layer, such that the generated holes can be blocked [125,126]. Similarly, the material for the hole transport layer (HTL) must be selected such that the valance band maxima of the material must be in the proper position to receive the photogenerated holes and the conduction band must be at a high position to stop the photogenerated electrons. In order to attain higher efficiency, proper band alignment between the perovskite layer and CTLs must be done. Energy band tuning is the sole field of the study conducted in

the PSCs to attain the best possible performance [127]. The proper energy band tuning ensures minimal interfacial recombination [128]. Apart from proper band alignment of the CTL other properties such as thermal stability, chemical reactivity, etc. impact the performance of the cell to a great extent. Defect passivation is another important strategy to overcome the issue of stability. Certain defect passivation techniques such as interlayer engineering, perovskite film formation conditions, film post-treatment, grain boundary passivation and more are being used by the researchers. The intrinsic stability of the perovskite film is attributed to the crystallographic and molecular structure of the material. The lattice imperfections within the material are dependent on stoichiometry, annealing time, annealing temperature, film deposition method, deposition time, and more [129]. The existence of the defects is determined by the defect formation energy of the material. All the above-stated conditions decide the defect formation energy of the material. Apart from the synthesis conditions, external factors such as moisture, heat, temperature, oxygen, etc. lead to the formation of the new defects during the operation of the PSCs, which in turn has a degrading impact [130]. This rapid degradation of the PSCs has hampered the commercialization of the PSCs despite attaining good performance.

4.2. Commercialization of PSCs

Long-term device stability is a vital parameter to determine the commercialization of PSCs. The device stability is evaluated in terms of device lifetime tested under 1-sun illumination at electric load. However, PSCs have not attained stability comparable to Si PVs because of their van der Waals interaction causing ion immigration, photo-degradation and phase segregation. Further, the poor intrinsic stability and soft ion lattice due to weak H-bond lead to poor stability.

The various commercialization companies are Oxford PV GmbH (Brandenburg, Germany), Swift solar (Sancarlos, CA, USA), Solaronix (Aubonne, Switzerland), Saule Technology (Wroclaw, Poland), Microquanta Semiconductor (Hangzhou, China) etc. [131]. Oxford PV developed the world's first full-size 100MW production line [132]. Many commercial companies in China and other countries are working on industrialization of PSCs such as GCL perovskites, Microquanta and a few more. Table 3 summarizes the details of the large-scale PSC modules. One potential issue for perovskite solar cells is the scalability needed for commercialization. The spin-coating method used for the majority of laboratory-scale tests is not effective for producing large-scale uniform coatings. This is because of the lack of consistency in film thickness over a large area, large material waste and lack of compatibility with the roll-to-roll processing that has a high throughput [133,134]. Industrial-scale techniques such as screen printing and slot-die coating have been identified as the most promising solutions to this [135]. They have already been used successfully to fabricate modules over 100 cm^2.

Table 3. Details of large-scale PSC modules fabricated by various companies or institutions.

Company/Institution Name	Country	PCE	Details	Module Area	Reference
Oxford Photovoltaics	United Kingdom	29.52%	Silicon-perovskite bifacial tandem cell	1 cm^2 per cell	[136]
Kaunas University of Technology	Lithuania	23.9%	Using spin coating	26 cm^2 active area of module	[137]
Saule Technology	Poland	10.2%	Doctor blade coating	15.7 cm^2 flexible module	[138]
Imec	Belgium	18.6%	Perovskite solar cell	16 cm^2 module	[139]
NEDO and Panasonic	Japan	16.09%	Using inkjet printing	802 cm^2 module	[140]
Toshiba and NEDO	Japan	11.7%	Perovskite solar cell (adjusting crystal growth)	703 cm^2 module	[141]
Solliance	Netherland	14.5%	Using the slot die coating	144 cm^2 per cell	[142]
Chinese Academy of Science (CAS)	China	19.2%	Using the slot die coating	16 cm^2 module	[143]
Microquanta	China	24.1%	Perovskite solar cell	20 cm^2 module	[144]

4.3. Future Outlook

For more than half a century, silicon PV technology dominates the largest PV market. Studies suggest that in order to obtain the highest efficiency from tandem cells, a wide bandgap perovskite material of bandgap of order 1.7 eV with a thickness of the order of 1 µm must be used. The synthesis of such perovskite material is a hot topic of research among the researchers of the PV community. If a perovskite material of bandgap 1.7 eV is obtained, then extracted voltage will reach about 1.3 V rendering the overall voltage of the device to be 2.0 V. In order to extract similar currents from both the cells, the thickness of the perovskite material must be of order 1 µm with a bandgap of about 1.7 eV. However, preparing high-quality microns-thick perovskite material is still a challenge. Another way to enhance the efficiency of the solar cells is to modify the tunnel junction material [145]. The widely used transparent conductive oxide (TCO) is indium tin oxide (ITO). ITOs are not considered ideal due to their improper transmissivity. The ITOs exhibit parasitic absorption at a range of 800 nm [146]. An ideal tunnelling junction must have high conductance and high transmittance in order to minimize recombination loss. An appropriate refractive index and thickness are also important to minimize the anisotropic conductance, and internal reflection and avoid lateral breakdown. It can be said that industrialization of tandem cells is completely dependent upon the development of perovskite materials.

Currently, state-of-the-art perovskite solar cells still require the use of lead (Pb^{2+}) as the B-cation site. Lead is a toxic element and its use could present problems if released into the environment, eventually working its way into the human food chain [147]. Therefore, a large amount of research has been conducted into alternative lead-free perovskite materials. Perovskite solar cells based on different elements such as antimony, copper, germanium, bismuth and others have all been tested [148–152]. The strongest candidate appears to be tin, having both a similar ionic radius and electronic configuration. This allows direct replacement of the lead ion in the B-site without a significant phase change. Tin-based perovskite cells have a PCE of around 10–12%, which is significantly lower than lead-containing perovskites [153,154]. It is also important to make sure that environmental burden-shifting is not taking place, as studies have found the oxidation of Sn^{2+} to Sn^{4+} can lead to the formation of toxic by-product hydroiodic acid [155]. Overall, Ju et al. state that only once the degradation and toxicity mechanisms of current perovskites are understood will lead-free, stable perovskites be fabricated [156]. Single-junction perovskite solar cells are not the only technology that has seen a large jump in PCE over the previous decade.

Tandem solar cells involving perovskite have been developed and are not constrained to the single-junction Shockley–Quessier limit. The efficiency limit for a tandem solar cell is 47%, much higher than the 31% for single-junction [157,158]. This is possible as Tandem solar cells better utilize small wavelength radiation from the spectrum. The tandem cell will have a top layer with a large bandgap material; this will absorb the short wavelength part of the spectrum. The longer wavelength radiation will pass through the top layer and be absorbed by the smaller band-gap bottom layer [159]. Perovskites can be combined with a variety of materials to create two-terminal tandem cells. Perovskite-Silicon has shown good performance reaching a PCE of 29.15%, outperforming the highest achieving monocrystalline silicon cell [160]. Perovskite–Perovskite cells have reached an impressive PCE of 24.8% [161]. Another successful combination of materials is perovskite with second-generation material CIGS, achieving 24.2% [162]. Overall, the high theoretical efficiency of tandem perovskite solar cells is predicted to allow the price of PV to continue to fall over the coming decades [163].

Two-dimensional (2D) Perovskites have also been explored as light absorbers for solar cells due to their wide structural diversity and superior stability compared to conventional 3D perovskites [164]. 2D perovskites are produced by using larger ammonium or diammonium cations. These cations are too large and divide the perovskite structure into 2D layers. The layered structures are placed into several categories, with Ruddlesden–Popper (RP) and Dion–Jacobson (DJ) being by far the most common [165–168]. RP structures are stacked so that they have two offset layers per unit cell having pairs of monovalent interlayer spacer cations. DJ structures can be stacked directly on top of each other and only require one divalent interlayer spacer per formula unit [169]. A successful example of a RP 2D-perovskite $(PEA)_2(MA)_2[Pb_3I_{10}]$ was synthesized and showed excellent resistance to moisture and allowed high-quality films to be produced after just 1-step [170,171]. However, this material only achieved a PCE of 4.73% [172]. Further improvement of the efficiency was made by improving the charge transport mechanism, reaching a PCE of 12.52% [173]. Although, 2D-perovskites show excellent stability they still lack the efficiency of 3D-perovskite cells. For this reason, they are not suitable for single-junction cells but may be an excellent option for use as the high band-gap absorber in a tandem cell [174]. The applications of perovskite material in PV involve usage in electric vehicles and building integrated technology because of its flexibility and tunable bandgap [175,176]. The increment in stability and performance enables the researchers to work not only on performance enhancement but to seek new applications as well. The proper surface engineering and interface engineering improved the efficiency and stability to a great extent. The performance improvement occurred due to a reduction in defect density within the material leading to a decrement in non-radiative recombination. The performance of PSCs is further improved by the surface passivation using hydrophobic molecules. Liang et al. used organic hydrophobic molecules (Benzylamine) with a side chain to enhance the performance of Formamidinium lead iodide (FAPbI3) films. This modification not only enhanced the voltage from 1 to 1.12 V but the stability improved from three days to four months [177,178]. It can be said that depositing high-quality perovskite film with minimum defects can enhance the performance of the PSCs.

Building integration of perovskite-based PV is probably one of the promising approaches. Building energy currently consumes significant energy which must be reduced by employing an energy-positive building envelope [179–183]. For decades, PV technology is placed in a building in terms of roof integrated or wall integrated technology. These are mainly known as building attached or applied PV. Building integrated type PV application semitransparent PV is a precondition [184,185]. However, previously most investigation was devoted based on first-generation silicon [186–188] or second-generation thin film-based PV [189–191]. However, the booming Perovskite industry gives high hope for the building industry [192,193]. Perovskite which can have variable [194] or static [195] transparency is the most suitable for building window or façade applications. The recent trend is to include a smart switchable or adaptive window in a building [196–203]. However,

these most effective windows can only reduce energy consumption [204–208]. In the future, switchable perovskite can be a dominant player in the building industry which can have the potential to generate benign electricity and also tune the transparency concomitantly.

5. Summary

The strive to generate electricity from renewable energy sources has highlighted the importance of using the abundant solar resources incident on the Earth. Photovoltaics are used to generate electricity using the photovoltaic effect. As solar PV capacity continues to increase across the globe, research has focused on maximizing the efficiency and decreasing the manufacturing costs of solar cells. Third-generation solar cells are currently in development and have great potential to dominate the solar PV market in the future. The most promising candidate identified is perovskite solar cells, reaching a PCE of 25.8% in under 10 years. Other features such as low material and processing costs make them an exciting development and the focus of this review.

The key structural and fundamental features that make perovskites such effective solar cells have been identified in this review. The structure of perovskite allows elements within it to be interchanged, as long as it stays within the Goldsmith tolerance factor. This provides great flexibility and also an ability to easily tune the bandgap of the material to a required value. Perovskite materials also have high efficiencies in photovoltaic applications. Key electronic and optical properties responsible for this include high electron mobility (800 cm^2/Vs), long diffusion wavelength (>1 μm), and high absorption coefficient (10^5 cm^{-1}). This review also discussed solution-processing and vapor deposition techniques for manufacturing perovskite solar cells. The most cost-effective and common method was solution-processing as vapor deposition requires expensive high vacuum levels for thermal evaporation. Overall, a one-step solution-based method was identified as the most effective. This allows grain growth to be controlled more effectively, resulting in a higher PCE.

There are still some major issues stopping large-scale commercialization of perovskite solar cells. The first is the stability of perovskite solar cells, they are inherently sensitive to light, heat, moisture, and oxygen. These issues must be addressed in order for perovskite solar cells to have a long operational lifetime competitive with silicon-based solar cells. Another issue facing perovskites is the current manufacturing techniques used in lab-scale projects are not suitable for large-scale production. This is being addressed with a search for techniques that are compatible with roll-to-roll processing allowing high throughput.

Finally, this paper addresses where future research should focus its attention. The first suggestion is to investigate lead-free perovskites, due to the negative impacts of lead-use. The most promising results have been found for tin-based perovskites achieving a PCE of 10–12%. Unfortunately, this cannot compete with lead-based perovskites that achieved PCE of 25% so further research is needed. The final topic addressed is tandem and multijunction cells, which capture a larger range of radiation from the spectrum. Not only do tandem cells increase the PCE, but also address the stability issues of perovskite cells. A perovskite-silicon tandem cell was synthesized and achieved a high PCE of 29.15%. Tandem cells involving 2D-perovskites as the high band-gap absorber have the potential to achieve a high PCE along with excellent stability. Overall, this review demonstrates the impressive features of perovskite solar cells along with the challenges that must be overcome for large-scale commercialization.

Author Contributions: Conceptualization, P.R. and A.G.; methodology, P.R. and A.G.; validation, P.R.; formal analysis, P.R.; investigation, A.K.; resources, A.K.; data curation, F.B.; writing—original draft preparation, F.B., P.R. and A.G.; writing—review and editing, F.B., P.R., A.G. and E.C.; visualization, F.B. and A.G.; supervision, A.G.; project administration, A.G. All authors have read and agreed to the published version of the manuscript.

Funding: This research received no external funding.

Institutional Review Board Statement: Not applicable.

Informed Consent Statement: Not applicable.

Data Availability Statement: Not applicable.

Conflicts of Interest: The authors declare no conflict of interest.

References

1. Nayak, P.K.; Mahesh, S.; Snaith, H.J.; Cahen, D. Photovoltaic solar cell technologies: Analysing the state of the art. *Nat. Rev. Mater.* **2019**, *4*, 269–285. [CrossRef]
2. Kabir, E.; Kumar, P.; Kumar, S.; Adelodun, A.A.; Kim, K.-H. Solar energy: Potential and future prospects. *Renew. Sustain. Energy Rev.* **2018**, *82*, 894–900. [CrossRef]
3. Lewis, N.S.; Nocera, D.G. Powering the planet: Chemical challenges in solar energy utilization. *PNAS* **2006**, *103*, 15729–15735. [CrossRef]
4. IRENA. Global Energy Transformation: A Roadmap to 2050 (2019 Edition). 2019. Available online: https://www.irena.org/publications/2019/Apr/Global-energy-transformation-A-roadmap-to-20502019Edition?-msclkid=a481d1f3a5fa11ec80aa03b73d80cbce (accessed on 17 March 2022).
5. Balkan Green Energy News, Global Solar Power to Cross 200 GW Annual Installation Threshold in 2022. 2021. Available online: https://balkangreenenergynews.com/global-solar-power-to-cross-200-gw-annual-installation-threshold-in-2022/?msclkid=880a2af4a60611ecbf2601d10dd12670 (accessed on 17 March 2022).
6. IRENA. Renewable Energy Technologies. 2020. Available online: https://www.irena.org/Statistics/View-Data-by-Topic/Capacity-and-Generation/Technologies (accessed on 17 March 2022).
7. Bagher, A.M.; Vahid, M.M.A.; Mohsen, M. Types of Solar Cells and Application. *Am. J. Opt. Photonics* **2015**, *3*, 94–113. [CrossRef]
8. Reddy, P.; Gupta, M.V.N.S.; Nundy, S.; Karthick, A.; Ghosh, A. Status of BIPV and BAPV System for Less Energy-Hungry Building in India—A Review. *Appl. Sci.* **2020**, *10*, 2337. [CrossRef]
9. Ghosh, A. Potential of building integrated and attached/applied photovoltaic (BIPV/BAPV) for adaptive less energy-hungry building's skin: A comprehensive review. *J. Cleaner. Prod.* **2020**, *276*, 123343. [CrossRef]
10. Envision2030: 17 Goals to Transform the World for Persons with Disabilities. 2022. Available online: https://www.un.org/development/desa/disabilities/envision2030.html (accessed on 29 May 2022).
11. Rappaport, P. The photovoltaic effect and its utilisation. *Sol. Energy* **1959**, *3*, 8–18. [CrossRef]
12. Kaushika, N.D.; Mishra, A.; Rai, A.K. *Solar Photovoltaics*; Springer Nature: Cham, Switzerland, 2019.
13. Shockley, W.; Queisser, H.J. Detailed Balance Limit of Efficiency of p-n Junction Solar Cells. *J. Appl. Phys.* **1961**, *32*, 510–519. [CrossRef]
14. Rühle, S. Tabulated values if the Shockley-Queisser limit for single junction solar cells. *Sol. Energy* **2016**, *130*, 139–147. [CrossRef]
15. IEA. Technology Roadmap–Solar Photovoltaic Energy 2010. 2010. Available online: https://www.iea.org/reports/technology-roadmap-solar-photovoltaic-energy-2010 (accessed on 22 February 2022).
16. Sharma, S.; Jain, K.K.; Sharma, A. Solar Cells: In Research and Applications—A Review. *Mater. Sci. Appl.* **2015**, *6*, 1145–1155. [CrossRef]
17. Yoshikawa, K.; Kawasaki, H.; Yoshida, W.; Irie, T.; Konishi, K.; Nakano, K.; Uto, T.; Adachi, D.; Kanematsu, M.; Uzu, H.; et al. Silicon heterojunction solar cell with interdigitated back contacts for a photoconversion efficiency over 26%. *Nat. Energy* **2017**, *2*, 17032. [CrossRef]
18. Sundaram, S.; Benson, D.; Mallick, T.K. Overview of the PV Industry and Different Technologies. In *Solar Photovoltaic Technology Production*; Elsevier: Amsterdam, The Netherlands, 2016; pp. 7–22.
19. Chopra, K.L.; Paulson, P.D.; Dutta, V. Thin-Film Solar Cells: An Overview. *Prog. Photovolt. Res. Appl.* **2004**, *12*, 69–92. [CrossRef]
20. Deshpande, R.A. Advances in Solar Cell Technology: An Overview. *J. Sci. Res.* **2021**, *65*, 1–4. [CrossRef]
21. Green, M.A.; Dunlop, E.D.; Hohl-Ebinger, J.; Yoshita, M.; Kopidakis, N.; Hao, X. Solar cell efficiency tables (Version 58). *Prog. Photovolt. Res. Appl.* **2021**, *29*, 657–667. [CrossRef]
22. Ossila. Organic Photovoltaics vs. 2nd-Generation Solar Cell Technologies. 2020. Available online: https://www.ossila.com/pages/organic-photovoltaics-vs-2nd-gen-solar-cell-tech (accessed on 22 February 2022).
23. Nakamura, M.; Yamaguchi, K.; Kimoto, Y.; Yasaki, Y.; Kato, T.; Sugimoto, H. Cd-Free Cu(In,Ga)(Se,S)$_2$ Thin-Film Solar Cell With Record Efficiency of 23.35%. *IEEE J. Photovolt.* **2019**, *9*, 1863–1867. [CrossRef]
24. Ragoussi, M.E.; Torres, T. New generation solar cells: Concepts, trends and perspectives. *Chem. Commun.* **2015**, *51*, 3957–3972. [CrossRef] [PubMed]
25. Das, K.K.; Reddy, R.C.; Bagoji, I.B.; Das, S.; Bagali, S.; Mullur, L.; Khodnapur, J.P.; Biradar, M.S. Primary concept of nickel toxicity–an overview. *J. Basic Clin. Physiol. Pharmacol.* **2018**, *30*, 141–152. [CrossRef]
26. Ong, K.H.; Agileswari, R.; Maniscalco, B.; Arnou, P.; Kumar, C.C.; Bowers, J.W.; Marsadek, M. Review on Substrate and Molybdenum Back Contact in CIGS Thin Film Solar Cell. *Int. J. Photoenergy* **2018**, *2018*, 1–14. [CrossRef]
27. Kojima, A.; Teshima, K.; Shirai, Y.; Miyasaka, T. Organometal Halide Perovskite as Visible-Light Sensitizers for Photovoltaic Cells. *J. Am. Chem. Soc.* **2009**, *131*, 6050–6605. [CrossRef] [PubMed]
28. Liu, Z.; Liu, P.; Li, M.; He, T.; Liu, T.; Yu, L.; Yuan, M. Efficient and Stable FA-Rich Perovskite Photovoltaics: From Material Properties to Device Optimization. *Adv. Energy Mater* **2022**, *12*, 2200111. [CrossRef]

29. Wang, R.; Huang, T.; Xue, J.; Tong, J.; Zhu, K.; Yang, Y. Prospects for metal halide perovskite-based tandem solar cells. *Nat. Photonics.* **2021**, *15*, 411–425. [CrossRef]
30. Corkish, R. Solar Cells. In *Encyclopedia of Energy*; Elsevier: Amsterdam, The Netherlands, 2004; pp. 545–557.
31. Saeed, M.A.; Cheng, S.; Biswas, S.; Kim, S.H.; Kwon, S.-K.; Kim, H.; Kim, Y.-H.; Shim, J.W. Remarkably high performance of organic photovoltaic devices with 3,9-bis(2-methylene-(3-(1,1-dicyanomethylene)-indanone))-5,5,11,11-tetrakis(4-hexyl metaphenyl)-dithieno [2,3-d:2′,3′-d′]-s-indaceno [1,2-b:5,6-b′]dithiophene)-ethylhexyloxy] photoactive ac. *J. Power Sources* **2022**, *518*, 230782. [CrossRef]
32. Saeed, M.A.; Kang, H.C.; Yoo, K.; Asiam, F.K.; Lee, J.-J.; Shim, J.W. Cosensitization of metal-based dyes for high-performance dye-sensitized photovoltaics under ambient lighting conditions. *Dye. Pigment.* **2021**, *194*, 109624. [CrossRef]
33. Alanazi, A.K. Effect of ZnO Nanomaterial and Red and Green Cabbage Dyes on the Performance of Dye-Sensitised Solar Cells. *Coatings* **2021**, *11*, 1057. [CrossRef]
34. Saeed, M.A.; Kim, S.H.; Kim, H.; Liang, J.; Woo, H.Y.; Kim, T.G.; Yan, H.; Shim, J.W. Indoor Organic Photovoltaics: Optimal Cell Design Principles with Synergistic Parasitic Resistance and Optical Modulation Effect. *Adv. Energy Mater.* **2021**, *11*, 2003103. [CrossRef]
35. Cao, J.; Yan, F. Recent progress in tin-based perovskite solar cells. *Energy Environ. Sci.* **2021**, *14*, 1286–1325. [CrossRef]
36. Nishimura, K.; Kamarudin, M.A.; Hirotani, D.; Hamada, K.; Shen, Q.; Iikubo, S.; Minemoto, T.; Yoshino, K.; Hayase, S. Hayase, Lead-free tin-halide perovskite solar cells with 13% efficiency. *Nano Energy* **2020**, *74*, 104858. [CrossRef]
37. Min, H.; Lee, D.Y.; Kim, J.; Kim, G.; Lee, K.S.; Kim, J.; Paik, M.J.; Kim, Y.K.; Kim, K.S.; Kim, M.G.; et al. Perovskite solar cells with atomically coherent interlayers on SnO_2 electrodes. *Nature* **2021**, *598*, 444–450. [CrossRef]
38. Quantum Dot Layer Pushes Perovskite Solar Cell Efficiency Up to 25.7%. 2022. Available online: https://www.pv-magazine.com/2022/01/24/quantum-dot-layer-pushes-perovskite-solar-cell-efficiency-up-to-25-7/ (accessed on 26 July 2022).
39. Azam, M.; Khan, A.; Liang, G.-X.; Li, G.-J.; Chen, S.; Zheng, Z.-H.; Farooq, U.; Ishaq, M.; Fan, P.; Wang, Z.; et al. Examining the Interfacial Defect Passivation with Chlorinated Organic Salt for Highly Efficient and Stable Perovskite Solar Cells. *Sol. RRL* **2020**, *4*, 2000358. [CrossRef]
40. Ghosh, A. Fenestration integrated BIPV (FIPV): A review. *Sol. Energy* **2022**, *237*, 213–230. [CrossRef]
41. Nundy, S.; Ghosh, A.; Mesloub, A.; Abdullah, G.; Mashary, M. Impact of COVID-19 pandemic on socio-economic, energy-environment and transport sector globally and sustainable development goal (SDG). *J. Clean. Prod.* **2021**, *312*, 127705. [CrossRef]
42. Snaith, H.J. Perovskite: The Emergence of a New Era for Low-Cost, High-Efficiency Solar Cells. *J. Phys. Chem. Lett.* **2013**, *4*, 3623–3630. [CrossRef]
43. Shi, J.; Guo, L. ABO3-based photocatalysts for water splitting. *Prog. Nat. Sci. Mater. Int.* **2013**, *22*, 592–615. [CrossRef]
44. Evans, H.A.; Wu, Y.; Seshadri, R.; Cheetham, A. Perovskite-related ReO3-type structures. *Nat. Rev. Mater.* **2020**, *5*, 196–213. [CrossRef]
45. Roy, A.; Ghosh, A.; Bhandari, S.; Sundaram, S.; Mallick, T. Perovskite Solar Cells for BIPV Application: A Review. *Buildings* **2020**, *10*, 129. [CrossRef]
46. Park, N.G. Halide perovskite photovoltaics: History, progress, and perspectives. *MRS Bull.* **2018**, *43*, 527–533. [CrossRef]
47. Park, N.G. Perovskite solar cells: An emerging photovoltaic technology. *Mater. Today* **2015**, *18*, 65–72. [CrossRef]
48. Bartel, C.J.; Sutton, C.; Goldsmith, B.R.; Ouyang, R.; Musgrave, C.B.; Ghiringhelli, L.M.; Scheffler, M. New tolerance factor to predict the stability of perovskite oxides and halides. *Sci. Adv.* **2019**, *5*, eaav0693. [CrossRef]
49. Goldsmith, V.M. Die Gesetze der Krystallochemie. *Naturwissenschaften* **1926**, *14*, 477–485.
50. Travis, W.; Glover, E.N.K.; Bronstein, H.; Scanlon, D.O.; Palgrave, R.G. On the application of the tolerance factor to inorganic and hybrid halide perovskites: A revised system. *Chem. Sci.* **2016**, *7*, 4548–4556. [CrossRef] [PubMed]
51. Hussain, I.; Tran, H.P.; Jaksik, J.; Moore, J.; Islam, N.; Uddin, M.J. Functional materials, device architecture, and flexibility of perovskite solar cell. *Emergent Mater.* **2018**, *1*, 133–154. [CrossRef]
52. Minemoto, T.; Murata, M. Theoretical analysis on effect of band offsets in perovskite solar cells. *Sol. Energy Mater. Sol. Cells* **2014**, *133*, 8–14. [CrossRef]
53. Roy, P.; Raoui, Y.; Khare, A. Design and simulation of efficient tin based perovskite solar cells through optimization of selective layers: Theoretical insights. *Opt. Mater.* **2022**, *125*, 112057. [CrossRef]
54. Roy, P.; Khare, A. Understanding the strategies to attain the best performance of all inorganic lead-free perovskite solar cells: Theoretical insights. *Int. J. Energy Res.* **2022**, 1–19. [CrossRef]
55. Elseman, A.M.; Sajid, S.; Shalan, A.E.; Mohamed, S.A.; Rashad, M.M. Recent progress concerning inorganic hole transport layers for efficient perovskite solar cells. *Appl. Phys. A Mater. Sci. Process.* **2019**, *125*, 1–12. [CrossRef]
56. Raj, A.; Kumar, M.; Anshul, A. Recent advancement in inorganic-organic electron transport layers in perovskite solar cell: Current status and future outlook. *Mater. Today Chem.* **2021**, *22*, 100595. [CrossRef]
57. Lavagna, L.; Syrrokostas, G.; Fagiolari, L.; Amici, J.; Francia, C.; Bodoardo, S.; Leftheriotis, G.; Bella, F. Platinum-free photoelectrochromic devices working with copper-based electrolytes for ultrastable smart windows. *J. Mater. Chem. A* **2021**, *9*, 19687–19691. [CrossRef]
58. Heydari Gharahcheshmeh, M.; Robinson, M.T.; Gleason, E.F.; Gleason, K.K. Optimizing the Optoelectronic Properties of Face-On Oriented Poly(3,4-Ethylenedioxythiophene) via Water-Assisted Oxidative Chemical Vapor Deposition. *Adv. Funct. Mater.* **2021**, *31*, 2008712. [CrossRef]

59. Kirchartz, T.; Kaienburg, P.; Baran, D. Figures of Merit Guiding Research on Organic Solar Cells. *J. Phys. Chem. C* **2018**, *122*, 5829–5843. [CrossRef]
60. Kim, J.Y.; Lee, J.W.; Jung, H.S.; Shin, H.; Park, N.G. High-Efficiency Perovskite Solar Cells. *Chem. Rev.* **2020**, *120*, 7867–7918. [CrossRef] [PubMed]
61. Bhandari, S.; Roy, A.; Ghosh, A.; Mallick, T.K.; Sundaram, S. Perceiving the temperature coefficients of carbon-based perovskite solar cells. Sustain. *Energy Fuels* **2020**, *4*, 6283–6298. [CrossRef]
62. Bhandari, S.; Roy, A.; Ghosh, A.; Mallick, T.K.; Sundaram, S. Performance of WO 3 -Incorporated Carbon Electrodes for Ambient Mesoscopic Perovskite Solar Cells. *ACS Omega* **2019**, *5*, 422–429. [CrossRef] [PubMed]
63. Miyata, A.; Mitioglu, A.; Plochocka, P.; Portugall, O.; Wang, J.T.-W.; Stranks, S.D.; Snaith, H.; Nicholas, R. Direct measurement of the exciton binding energy and effective masses for charge carriers in organic-inorganic tri-halide perovskite. *Nat. Phys.* **2015**, *11*, 582–587. [CrossRef]
64. Roy, P.; Sinha, N.K.; Tiwari, S.; Khare, A. A review of perovskite solar cells: Evolution of architecture, fabrication techniques, commercialization issues and status. *Sol. Energy* **2020**, *198*, 665–688. [CrossRef]
65. Im, J.-H.; Chung, J.; Kim, S.-J.; Park, N.-G. Synthesis, structure, and photovoltaic property of a nanocrystalline 2H perovskite-type novel sensitizer ($CH_3CH_2NH_3$)PbI_3. *Nanoscale Res. Lett.* **2012**, *7*, 353. [CrossRef] [PubMed]
66. Koh, T.M.; Fu, K.; Fang, Y.; Chen, S.; Sum, T.C.; Mathews, N.; Mhaisalkar, S.G.; Boix, P.P.; Baikie, T. Formamidinium-Containing Metal-Halide: An Alternative Material for Near-IR Absorption Perovskite Solar Cells. *J. Phys. Chem. C* **2013**, *118*, 16458–16462. [CrossRef]
67. Eperon, G.E.; Stranks, S.D.; Menelaou, C.; Johnston, M.B.; Herz, L.M.; Snaith, H.J. Formamidinium lead trihalide: A broadly tunable perovskite for efficient planar heterojunction solar cells. *Energy Environ. Sci.* **2014**, *7*, 982–988. [CrossRef]
68. Pellet, N.; Gao, P.; Gregori, G.; Yang, T.-Y.; Nazeeruddin, M.K.; Maier, J.; Grätzel, M. Mixed-Organic Cation Perovskite Photovoltaics for Enhanced Solar-Light Harvesting. *Angew. Chem.* **2014**, *126*, 3215–3221. [CrossRef]
69. Jeon, N.J.; Noh, J.H.; Yang, W.S.; Kim, Y.C.; Ryu, S.; Seo, J.; Seok, S.I. Compositional engineering of perovskite materials for high-performance solar cells. *Nature* **2015**, *517*, 476–480. [CrossRef]
70. Mosconi, E.; Amat, A.; Nazeeruddin, K.; Grätzel, M.; De Angelis, F. First Principles Modelling of Mixed Halide Organometal Perovskites for Photovoltaic Application. *J. Phys. Chem. C* **2013**, *117*, 13902–13913. [CrossRef]
71. Buin, A.; Comin, R.; Xu, J.; Ip, A.H.; Sargent, E.H. Halide-Dependent Electronic Structure of Organolead Perovskite Materials. *Chem. Mater.* **2015**, *27*, 4405–4412. [CrossRef]
72. Hu, M.; Bi, C.; Yuan, Y.; Bai, Y.; Huang, J. Stabilised Wide Bandgap MAPbBrxI3-x Perovskite by Enhanced Grain Size and Improved Crystallinity. *Adv. Sci.* **2015**, *3*, 1500301. [CrossRef]
73. Wu, T.; Liu, X.; Luo, X.; Lin, X.; Cui, D.; Wang, Y.; Segawa, H.; Zhang, Y.; Han, L. Lead-free tin perovskite solar cells. *Joule* **2021**, *5*, 863–886. [CrossRef]
74. Kopacic, I.; Friesenbichler, B.; Hoefler, S.F.; Kunert, B.; Plank, H.; Rath, T.; Trimmel, G. Enhanced Performance of Germanium Halide Perovskite Solar Cells through Compositional Engineering. *ACS Appl. Energy Mater.* **2018**, *1*, 343–347. [CrossRef]
75. Kumar, M.H.; Dharani, S.; Leong, W.L.; Boix, P.P.; Prabhakar, R.R.; Baikie, T.; Shi, C.; Ding, H.; Ramesh, R.; Asta, M.; et al. Lead-free halide perovskite solar cells with high photocurrents realized through vacancy modulation. *Adv. Mater.* **2014**, *26*, 7122–7127. [CrossRef]
76. Lee, B.; Stoumpos, C.C.; Zhou, N.; Hao, F.; Malliakas, C.; Yeh, C.; Marks, T.J.; Kanatzidis, M.G.; Chang, R.P.H. Air-Stable Molecular Semiconducting Iodosalts for Solar Cell Applications: Cs 2 SnI 6 as a Hole Conductor. *J. Am. Chem. Soc.* **2014**, *136*, 15379–15385. [CrossRef] [PubMed]
77. Noel, N.K.; Stranks, S.D.; Abate, A.; Wehrenfennig, C.; Guarnera, S.; Haghighirad, A.A.; Sadhanala, A.; Eperon, G.E.; Pathak, S.K.; Johnston, M.B.; et al. Lead-free organic–inorganic tin halide perovskites for photovoltaic applications. *Energy Environ. Sci.* **2014**, *7*, 3061–3068. [CrossRef]
78. Tai, Q.; Guo, X.; Tang, G.; You, P.; Ng, T.W.; Shen, D.; Cao, J.; Liu, C.K.; Wang, N.; Zhu, Y.; et al. Antioxidant Grain Passivation for Air-Stable Tin-Based Perovskite Solar Cells. *Angew. Chem.* **2019**, *58*, 806–810. [CrossRef]
79. Chen, M.; Ju, M.G.; Garces, H.F.; Carl, A.D.; Ono, L.K.; Hawash, Z.; Zhang, Y.; Shen, T.; Qi, Y.; Grimm, R.L.; et al. Highly stable and efficient all-inorganic lead-free perovskite solar cells with native-oxide passivation. *Nat. Commun.* **2019**, *10*, 1–8. [CrossRef]
80. Hao, F.; Stoumpos, K.; Cao, D.H.; Chang, R.P.H.; Kanatzidis, M. Lead-free solid-state organic-inorganic halide perovskite solar cells. *Nat. Photonics* **2014**, *8*, 489–494. [CrossRef]
81. Bansode, U.; Naphade, R.; Game, O.; Agarkar, S.; Ogale, S. Hybrid perovskite films by a new variant of pulsed excimer laser deposition: A roomerature dry process. *J. Phys. Chem. C* **2015**, *119*, 9177–9185. [CrossRef]
82. Shao, S.; Liu, J.; Portale, G.; Fang, H.H.; Blake, G.R.; ten Brink, G.H.; Koster, L.J.A.; Loi, M.A. Highly Reproducible Sn-Based Hybrid Perovskite Solar Cells with 9% Efficiency. *Adv. Energy Mater.* **2018**, *8*, 1702019. [CrossRef]
83. Jokar, E.; Chien, C.; Tsai, C.; Fathi, A.; Diau, E.W. Robust Tin-Based Perovskite Solar Cells with Hybrid Organic Cations to Attain Efficiency Approaching 10%. *Adv. Mater.* **2018**, *31*, 1804835. [CrossRef] [PubMed]
84. Zuo, F.; Williams, S.T.; Liang, P.W.; Chueh, C.C.; Liao, C.Y.; Jen, A.K.Y. Binary-Metal Perovskites Toward High-Performance Planar-Heterojunction Hybrid Solar Cells. *Adv Mater.* **2014**, *26*, 6454–6460. [CrossRef] [PubMed]
85. Chung, I.; Lee, B.; He, J.; Chang, R.P.H.; Kanatzidis, M.G. All-solid-state dye-sensitized solar cells with high efficiency. *Nature* **2012**, *485*, 486–489. [CrossRef]

86. Lee, S.; Kang, D. Highly Efficient and Stable Sn-rich Perovskite Solar Cells by Introducing Bromine Highly Efficient and Stable Sn-rich Perovskite Solar Cells by Introducing Bromine. *ACS Appl. Mater. Interfaces* **2017**, *9*, 22432–22439. [CrossRef] [PubMed]
87. Mohanty, I.; Mangal, S.; Udai, P.S. Performance optimization of lead free-MASnI3/CIGS heterojunction solar cell with 28.7% efficiency: A numerical approach. *Optical Materials* **2021**, *122*, 111812. [CrossRef]
88. Yang, Z.; Rajagopal, A.; Chueh, C.; Jo, S.B.; Liu, B.; Zhao, T.; Jen, A.K. Stable Low-Bandgap Pb–Sn Binary Perovskites for Tandem Solar Cells. *Adv. Mater.* **2016**, *28*, 8990–8997. [CrossRef]
89. Eperon, G.E.; Leijtens, T.; Bush, K.A.; Prasanna, R.; Green, T.; Wang, J.; McMeekin, D.P.; Volonakis, G.; Milot, R.L.; May, R.; et al. Perovskite-perovskite tandem photovoltaics with optimized band gaps. *Science* **2016**, *354*, 861–865. [CrossRef] [PubMed]
90. Liao, W.; Zhao, D.; Yu, Y.; Shrestha, N.; Ghimire, K.; Grice, C.R.; Wang, C.; Xiao, Y.; Cimaroli, A.J.; Ellingson, R.J.; et al. Fabrication of Efficient Low-Bandgap Perovskite Solar Cells by Combining Formamidinium Tin Iodide with Methylammonium Lead Iodide. *J. Am. Chem. Soc.* **2016**, *138*, 12360–12363. [CrossRef] [PubMed]
91. Wang, Z.K.; Li, M.; Yang, Y.G.; Hu, Y.; Ma, H.; Gao, X.Y.; Liao, L.S. High Efficiency Pb–In Binary Metal Perovskite Solar Cells. *Adv. Mater.* **2016**, *28*, 6695–6703. [CrossRef] [PubMed]
92. Fievez, M.; Rana, P.J.S.; Koh, T.M.; Manceau, M.; Lew, J.H.; Jamaludin, N.F.; Ghosh, B.; Bruno, A.; Cros, S.; Berson, S.; et al. Slot-die coated methylammonium-free perovskite solar cells with 18% efficiency. *Sol. Energy Mater. Sol. Cells* **2021**, *230*, 111–189. [CrossRef]
93. Ramirez, I.; Zhang, J.; Ducati, C.; Grovenor, C.; Johnston, M.B.; Ginger, D.S.; Nicholas, J.; Snaith, H.J. Environmental Science. *Energy Environ. Sci.* **2016**, *9*, 2892–2901.
94. Zheng, X.; Hou, Y.; Bao, C.; Yin, J.; Yuan, F.; Huang, Z.; Song, K.; Liu, J.; Troughton, J.; Gasparini, N.; et al. Managing grains and interfaces via ligand anchoring enables 22.3%-efficiency inverted perovskite solar cells. *Nat. Energy* **2020**, *5*, 131–140. [CrossRef]
95. Cacovich, S.; Vidon, G.; Degani, M.; Legrand, M.; Gouda, L.; Puel, J.; Vaynzof, Y.; Guillemoles, J.; Ory, D.; Grancini, G. Imaging and quantifying non-radiative losses at 23% efficient inverted perovskite solar cells interfaces. *Nat. Commun.* **2022**, *13*, 2868. [CrossRef] [PubMed]
96. Degani, M.; An, Q.; Albaladejo-Siguan, M.; Hofstetter, Y.J.; Cho, C.; Paulus, F.; Grancini, G.; Vaynzof, Y. 23.7% Efficient inverted perovskite solar cells by dual interfacial modification. *Sci. Adv.* **2021**, *7*, eabj7930. [CrossRef] [PubMed]
97. Jeong, M.J.; Yeom, K.M.; Kim, S.J.; Jung, E.H.; Noh, J.H. Spontaneous interface engineering for dopant-free poly(3-hexylthiophene) perovskite solar cells with efficiency over 24%. *Energy Environ. Sci.* **2021**, *14*, 2419–2428. [CrossRef]
98. Jeong, M.; Choi, I.W.; Go, E.M.; Cho, Y.; Kim, M.; Lee, B.; Jeong, S.; Jo, Y.; Choi, H.W.; Lee, J.; et al. Stable perovskite solar cells with efficiency exceeding 24.8% and 0.3-V voltage loss. *Science* **2020**, *369*, 1615–1620. [CrossRef]
99. Feng, X.; Guo, Q.; Xiu, J.; Ying, Z.; Ng, K.W.; Huang, L.; Wang, S.; Pan, H.; Tang, Z.; He, Z. Close-loop recycling of perovskite solar cells through dissolution-recrystallization of perovskite by butylamine. *Cell Reports Physical Science* **2021**, *2*, 100341. [CrossRef]
100. Li, H.; Zuo, C.; Scully, A.D.; Angmo, D.; Yang, J.; Gao, M. Recent progress towards roll-to-roll manufacturing of perovskite solar cells using slot-die processing. *Flex. Print. Electron.* **2020**, *5*, 014006. [CrossRef]
101. Ansari, M.I.H.; Qurashi, A.; Nazeeruddin, M.K. Frontiers, opportunities, and challenges in perovskite solar cells: A critical review. *J. Photochem. Photobiol. C* **2017**, *25*, 1–24. [CrossRef]
102. Liang, K.; Mitzi, D.B.; Prikas, M.T. Synthesis and Characterization of Organic-Inorganic Perovskite Thin Films Prepared Using a Versatile Two-Step Dipping Technique. *Chem. Mater.* **1998**, *10*, 403–411. [CrossRef]
103. Burschka, J.; Pellet, N.; Moon, S.J.; Humphry-Baker, R.; Gao, P.; Nazeeruddin, M.K.; Grätzel, M. Sequential deposition as a route to high-performance perovskite-sensitized solar cells. *Nature* **2013**, *499*, 316–320. [CrossRef]
104. Liu, M.; Johnston, M.B.; Snaith, H.J. Efficient planar heterojunction perovskite solar cells by vapour deposition. *Nature* **2013**, *501*, 395–398. [CrossRef]
105. Cui, J.; Yuan, H.; Li, J.; Xu, X.; Shen, Y.; Lin, H.; Wang, M. Recent progress in efficient hybrid lead halide perovskite solar cells. *Sci. Technol. Adv. Mater.* **2015**, *16*, 36004. [CrossRef] [PubMed]
106. Chen, Q.; Zhou, H.; Hong, Z.; Luo, S.; Duan, H.S.; Wang, H.H. Planar Heterojunction Perovskite Solar Cells via Vapor-Assisted Solution Process. *J. Am. Chem. Soc.* **2013**, *136*, 622–625. [CrossRef]
107. Smecca, E.; Valenzano, V.; Valastro, S.; Deretzis, I.; Mannino, G.; Malandrino, G.; Accorsi, G.; Colella, S.; Rizzo, A.; La Magna, A.; et al. Two-step MAPbI 3 deposition by low-vacuum proximity-space-effusion for high-efficiency inverted semitransparent perovskite solar cells. *J. Mater. Chem. A* **2021**, *9*, 16456–16469. [CrossRef]
108. Vesce, L.; Stefanelli, M.; Herterich, J.P.; Castriotta, L.A.; Kohlstädt, M.; Würfel, U.; Di Carlo, A. Ambient Air Blade-Coating Fabrication of Stable Triple-Cation Perovskite Solar Modules by Green Solvent Quenching. *Sol. RRL* **2021**, *5*, 2100073. [CrossRef]
109. He, M.; Li, B.; Cui, X.; Jiang, B.; He, Y.; Chen, Y.; O'Neil, D.; Szymanski, P.; Ei-Sayed, M.A.; Huang, J.; et al. Meniscus-assisted solution printing of large-grained perovskite films for high-efficiency solar cells. *Nat. Commun.* **2017**, *8*, 16045. [CrossRef]
110. Huang, H.H.; Liu, Q.H.; Tsai, H.; Shrestha, S.; Su, L.Y.; Chen, P.T.; Chen, Y.T.; Yang, T.A.; Lu, H.; Chuang, C.H.; et al. A simple one-step method with wide processing window for high-quality perovskite mini-module fabrication. *Joule* **2021**, *5*, 958–974. [CrossRef]
111. Hamukwaya, S.L.; Hao, H.; Zhao, Z.; Dong, J.; Zhong, T.; Xing, J.; Hao, L.; Mashingaidze, M.M. Review of Recent Developments in Preparation Methods for Large-Area Perovskite Solar Cells. *Coatings* **2022**, *12*, 252. [CrossRef]
112. Oxford PV, The Perovskite-on-Silicon Tandem Cell. 2022. Available online: https://www.oxfordpv.com/perovskite-silicon-tandem-cell (accessed on 5 July 2022).

113. Raza, E.; Ahmad, Z. Review on two-terminal and four-terminal crystalline-silicon/perovskite tandem solar cells; progress, challenges, and future perspectives. *Energy Rep.* **2022**, *8*, 5820–5851. [CrossRef]
114. Al-Ashouri, A.; Köhnen, E.; Li, B.; Magomedov, A.; Hempel, H.; Caprioglio, P.; Márquez, J.A.; Morales Vilches, A.B.; Kasparavicius, E.; Smith, J.A.; et al. Albrecht, Monolithic perovskite/silicon tandem solar cell with >29% efficiency by enhanced hole extraction. *Science* **2020**, *370*, 1300–1309. [CrossRef] [PubMed]
115. Li, N.; Niu, X.; Chen, Q.; Zhou, H. Towards commercialization: The operational stability of perovskite solar cells. *Chem. Soc. Rev.* **2020**, *49*, 8235–8286. [CrossRef]
116. Wu, T.; Qin, Z.; Wang, Y.; Wu, Y.; Chen, W.; Zhang, S.; Cai, M.; Dai, S.; Zhang, J.; Liu, J.; et al. The Main Progress of Perovskite Solar Cells in 2020–2021. *Nano-Micro Lett.* **2021**, *13*, 152. [CrossRef]
117. El-Mellouhi, F.; Marzouk, A.; Bentria, E.T.; Rashkeev, S.N.; Kais, S.; Alharbi, F.H. Hydrogen Bonding and Stability of Hybrid Organic-Inorganic Perovskites. *ChemSusChem* **2016**, *9*, 2648–2655. [CrossRef] [PubMed]
118. Niu, G.; Li, W.; Meng, F.; Wang, L.; Dong, H.; Qiu, Y. Study on the stability of CH3NH3PbI3 films and the effect of post-modification by aluminium oxide in all-solid-state hybrid solar cells. *J. Mater. Chem.* **2013**, *2*, 705–710. [CrossRef]
119. Lu, H.; Krishna, A.; Zakeeruddin, S.M.; Grätzel, M.; Hagfeldt, A. Compositional and Interface Engineering of Organic-Inorganic Lead Halide Perovskite Solar Cells. *IScience* **2020**, *23*, 101359. [CrossRef]
120. Yin, W.-J.; Shi, T.; Yan, Y. Unusual defect physics in $CH_3NH_3PbI_3$ perovskite solar cell absorber. *Appl. Phys. Lett.* **2014**, *104*, 063903. [CrossRef]
121. Amat, A.; Mosconi, E.; Ronca, E.; Quarti, C.; Umari, P.; Nazeeruddin, M.K.; Grätzel, M.; De Angelis, F. Cation-Induced Band-Gap Tuning in Organohalide Perovskites: Interplay of Spin–Orbit Coupling and Octahedra Tilting. *Nano Lett.* **2014**, *14*, 3608–3616. [CrossRef]
122. Poespawati, N.R.; Sulistianto, J.; Abuzairi, T.; Purnamaningsih, R.W. Performance and Stability Comparison of Low-Cost Mixed Halide Perovskite Solar Cells: $CH_3NH_3PbI_3$. *Int. J. Photoenergy* **2020**, *2020*, 1–10. [CrossRef]
123. Juarez-Perez, E.J.; Hawash, Z.; Raga, S.R.; Ono, L.K.; Qi, Y. Thermal degradation of $CH_3NH_3PbI_3$ perovskite into NH_3 and CH_3I gases observed by coupled thermogravimetry–mass spectrometry analysis. *Energy Environ. Sci.* **2016**, *9*, 3406–3410. [CrossRef]
124. Peng, Z.; Wei, Q.; Chen, H.; Liu, Y.; Wang, F.; Jiang, X.; Liu, W.; Zhou, W.; Ling, S.; Ning, Z. $Cs_{0.15}FA_{0.85}PbI_3/Cs_xFA_{1-x}PbI_3$ Core/Shell Heterostructure for Highly Stable and Efficient Perovskite Solar Cells. *Cell Rep. Phys. Sci.* **2020**, *1*, 100224. [CrossRef]
125. Mazumdar, S.; Du, B.; Huang, C.; Lin, P.; Zhao, J.; Zeng, X.; Ke, S. electron transporting layer for efficient perovskite solar cell by deliberating over nano-electrical conductivity. *Sol. Energy Mater. Sol. Cells* **2019**, *200*, 109995. [CrossRef]
126. Wang, S.; Li, X.; Tong, T.; Han, J.; Zhang, Y.; Zhu, J.; Huang, Z.; Choy, W.C. Sequential Processing: Spontaneous Improvements in Film Quality and Interfacial Engineering for Efficient Perovskite Solar Cells. *Sol. RRL* **2018**, *2*, 1800027. [CrossRef]
127. Prasanna, R.; Gold-Parker, A.; Leijtens, T.; Conings, B.; Babayigit, A.; Boyen, H.G.; Toney, M.F.; McGehee, M.D. Band Gap Tuning via Lattice Contraction and Octahedral Tilting in Perovskite Materials for Photovoltaics. *J. Am. Chem. Soc.* **2017**, *139*, 11117–11124. [CrossRef] [PubMed]
128. Zhang, M.; Chen, Q.; Xue, R.; Zhan, Y.; Wang, C.; Lai, J.; Yang, J.; Lin, H.; Yao, J.; Li, Y.; et al. Reconfiguration of interfacial energy band structure for high-performance inverted structure perovskite solar cells. *Nat. Commun.* **2019**, *10*, 4593. [CrossRef]
129. Mazumdar, S.; Zhao, Y.; Zhang, X. Stability of Perovskite Solar Cells: Degradation Mechanisms and Remedies. *Front. Electron.* **2021**, *2*. [CrossRef]
130. Pearson, A.J.; Eperon, G.E.; Hopkinson, P.E.; Habisreutinger, S.N.; Wang, J.T.; Snaith, H.J.; Greenham, N.C. Oxygen Degradation in Mesoporous Al_2O_3 /$CH_3NH_3PbI_{3-x}Cl_x$ Perovskite Solar Cells: Kinetics and Mechanisms. *Adv. Energy Mater.* **2016**, *6*, 1600014. [CrossRef]
131. Liu, H.; Zhang, Z.; Yang, F.; Yang, J.; Grace, A.N.; Li, J.; Tripathi, S.; Jain, S.M. Dopants for enhanced performance of tin-based perovskite solar cells—a short review. *Coatings* **2021**, *11*, 1045. [CrossRef]
132. PV Magazine, Oxford PV Completes 100 MW Factory Build Out. 2021. Available online: https://www.pv-magazine.com/2021/07/23/oxford-pv-completes-100-mw-factory-build-out/ (accessed on 5 July 2022).
133. Kim, Y.Y.; Yang, T.Y.; Suhonen, R.; Välimäki, M.; Maaninen, T.; Kemppainen, A.; Jeon, N.J.; Seo, J. Gravure-Printed Flexible Perovskite Solar Cells: Towards Roll-to-Roll Manufacturing. *Adv. Sci.* **2019**, *6*, 1802094. [CrossRef]
134. Dou, B.; Whitaker, J.B.; Bruening, K.; Moore, D.T.; Wheeler, L.M.; Ryter, J.; Breslin, N.J.; Berry, J.J.; Garner, S.M.; Barnes, F.S.; et al. Roll-to-Roll Printing of Perovskite Solar Cells. *ACS Energy Lett.* **2018**, *3*, 2558–2565. [CrossRef]
135. Rong, Y.; Ming, Y.; Ji, W.; Li, D.; Mei, A.; Hu, Y. Toward Industrial-Scale Production of Perovskite Solar Cells: Screen Printing, Slot-Die Coating, and Emerging Techniques. *J. Phys. Chem. Lett.* **2018**, *9*, 2707–2713. [CrossRef] [PubMed]
136. Breaking Efficiency Records with Tandem Solar Cells. 2022. Available online: https://www.chemistryworld.com/news/breaking-efficiency-records-with-tandem-solar-cells/4015529.article (accessed on 29 May 2022).
137. Liu, C.; Yang, Y.; Rakstys, K.; Mahata, A.; Franckevicius, M.; Mosconi, E.; Skackauskaite, R.; Ding, B.; Brooks, K.G.; Usiobo, O.J.; et al. Tuning structural isomers of phenylenediammonium to afford efficient and stable perovskite solar cells and modules. *Nat. Commun.* **2021**, *12*, 6394. [CrossRef]
138. Researchers at CHOSE and Saule Technologies Design a Large-Area Flexible Perovskite Solar Module Using a Fully Scalable Deposition Technique. 2021. Available online: https://www.perovskite-info.com/researchers-chose-and-saule-technologies-design-large-area-flexible-perovskite (accessed on 29 May 2022).

139. Imec Realizes 18.6% Efficient Perovskite Solar Cell. 2021. Available online: https://www.electronicsforu.com/technology-trends/research-papers/imec-realizes-18-6-efficient-perovskite-solar-cell (accessed on 29 May 2022).
140. Japan's NEDO and Panasonic Achieve 16.09% Efficiency for Large-Area Perovskite Solar Cell Module. 2020. Available online: https://www.perovskite-info.com/japan-s-nedo-and-panasonic-achieve-1609-efficiency-large-area-perovskite-solar (accessed on 29 May 2022).
141. Saule Technologies on Its Way to Launching Prototype Production Line in Q4 2019. Available online: https://www.perovskite-info.com/saule-technologies-its-way-launching-prototype-production-line-q4-2019 (accessed on 29 May 2022).
142. Great Cell Unveils Its Perovskite-Based Solar Cells Commercialization Roadmap 2018. Available online: https://www.perovskite-info.com/greatcell-unveils-its-perovskite-based-solar-cells-commercialization-roadmap (accessed on 29 May 2022).
143. Du, M.; Zhu, X.; Wang, L.; Wang, H.; Feng, J.; Jiang, X.; Cao, Y.; Sun, Y.; Duan, L.; Jiao, Y.; et al. High-Pressure Nitrogen-Extraction and Effective Passivation to Attain Highest Large-Area Perovskite Solar Module Efficiency. *Adv. Mater.* **2020**, *32*, 2004979. [CrossRef] [PubMed]
144. Chinese PV Industry Brief: Microquanta Builds 12 MW Ground-Mounted Project with Perovskite Solar Modules. 2022. Available online: https://www.pv-magazine.com/2022/02/18/chinese-pv-industry-brief-microquanta-builds-12-mw-ground-mounted-project-with-perovskite-solar-modules (accessed on 29 May 2022).
145. Qiang, Z.; Wang, C.; Gao, X.; Zhao, X.; Tian, H.; Wang, W.; Zong, J.; Fan, J. Challenges of Scalable Development for Perovskite/Silicon Tandem Solar Cells. *ACS Appl. Energy Mater.* **2022**, *5*, 6499–6515. [CrossRef]
146. Albrecht, S.; Saliba, M.; Baena, J.P.C.; Lang, F.; Kegelmann, L.; Mews, M.; Steier, L.; Abate, A.; Rappich, J.; Korte, L.; et al. Monolithic perovskite/silicon-heterojunction tandem solar cells processed at low temperature. *Energy Environ. Sci.* **2016**, *9*, 81–88. [CrossRef]
147. Florence, T.M.; Lilley, S.G.; Stauber, J.L. Skin Absorption of Lead. *Lancet* **1988**, *332*, 157–158. [CrossRef]
148. Saparov, B.; Hong, F.; Sun, J.P.; Duan, H.S.; Meng, W.; Cameron, S. Thin-Film Preparation and Characterisation of Cs3Sb2I9: A Lead-Free Layered Perovskite Semiconductor. *Chem. Mater.* **2015**, *27*, 5622–5632. [CrossRef]
149. Cortecchia, D.; Dewi, H.A.; Yin, J.; Bruno, A.; Chen, S.; Baikie, T.; Boix, P.P.; Grätze, M.; Mhaisalkar, S.; Soci, C.; et al. Lead-Free $MA_2CuCl_xBr_{4-x}$ Hybrid Perovskites. *Inorg. Chem.* **2016**, *55*, 1044–1052. [CrossRef]
150. Krishnamoorthy, T.; Ding, H.; Yan, C.; Leong, W.L.; Baikie, T.; Zhang, Z. Lead-free germanium iodide perovskite materials for photovoltaic applications. *J. Mater. Chem. A* **2015**, *3*, 23829–23832. [CrossRef]
151. Shao, Z.; Mercier, T.L.; Madec, M.B.; Pauporté, T.H. Exploring AgBixI3x+1 semiconductor thin films for lead-free perovskite solar cells. *Mater. Des.* **2017**, *141*, 81–87. [CrossRef]
152. Heydari Gharahcheshmeh, M.; Gleason, K.K. Recent Progress in Conjugated Conducting and Semiconducting Polymers for Energy Devices. *Energies* **2022**, *15*, 3661. [CrossRef]
153. Wu, T.; Liu, X.; He, X.; Wang, Y.; Meng, X.; Noda, T.; Yang, X.; Han, L. Efficient and stable tin-based perovskite cells by introducing π-conjugated Lewis base. *Sci. China: Chem.* **2019**, *63*, 107–115. [CrossRef]
154. Nakamura, T.; Yakumaru, S.; Truong, M.A.; Kim, K.; Liu, J.; Hu, S.; Otsuka, K.; Hashimoto, R.; Murdey, R.; Sasamori, T.; et al. Sn(IV)-free tin perovskite films realized by in situ Sn(0) nanoparticle treatment of the precursor solution. *Nat. Commun.* **2020**, *11*, 3008. [CrossRef] [PubMed]
155. Babayigit, A.; Ethirajan, A.; Muller, M.; Conings, B. Toxicity of organometal halide perovskite solar cells. *Nat. Mater.* **2016**, *15*, 247–251. [CrossRef]
156. Ju, M.G.; Chen, M.; Zhou, Y.; Dai, J.; Ma, L.; Padture, N.P.; Zeng, X.C. Towards Eco-friendly and Stable Perovskite Materials for Photovoltaics. *Joule* **2018**, *2*, 1231–1241. [CrossRef]
157. Brown, A.S.; Green, M.A. Detailed balance limit for the series constrained two terminal tandem solar cell. *Phys. E* **2002**, *14*, 96–100. [CrossRef]
158. Bremner, S.P.; Levy, M.Y.; Honsberg, C.B. Analysis of Tandem Solar Cell Efficiencies Under AM1.5G Spectrum Using a Rapid Flux Calculation Method. *Prog. Photovolt. Res. Appl.* **2007**, *16*, 225–233. [CrossRef]
159. Lal, N.N.; Dkhissi, Y.; Li, W.; Hou, Q.; Cheng, Y.B.; Bach, U. Perovskite Tandem Solar Cells. *Adv. Energy. Mater.* **2017**, *7*, 1602761. [CrossRef]
160. Hutchins, M. Tandem Cells Approaching 30% Efficiency. 2020. Available online: https://www.pv-magazine.com/2020/01/30/tandems-cells-approaching-30efficiency/?msclkid=cd9b65a8ab8811ec96d950d8a6454dce (accessed on 24 March 2022).
161. Lin, R.; Xiao, K.; Qin, Z.; Han, Q.; Zhang, C.; Wei, M. Monolithic all-perovskite tandem solar cells with 24.8% efficiency exploiting comproportionation to supress Sn(II) oxidation in precursor ink. *Nat. Energy.* **2019**, *4*, 864–873. [CrossRef]
162. Hutchins, M. HZB Hits 23.26% Efficiency with CIGS-Perovskite Tandem Cell. 2019. Available online: https://www.pv-magazine.com/2019/09/11/hzb-hits-23-26-efficiency-with-cigs-perovskite-tandem-cell/ (accessed on 24 March 2022).
163. Heo, J.H.; Im, S.H. CH3NH3PbBr3-CH3NH3PbI3 Perovskite-Perovskite Tandem Solar Cells with Exceeding 2.2V Open Circuit Voltage. *Adv. Mater.* **2015**, *28*, 5121–5125. [CrossRef] [PubMed]
164. Li, X.; Hoffman, J.; Ke, W.; Chen, M.; Tsai, H.; Nie, W.; Mohite, A.D.; Kepenekian, M.; Katan, C.; Even, J.; et al. Two-Dimensional Halide Perovskite Incorporating Straight Chain Symmetric Diammonium Ion, $(NH_3CmH_2mNH_3)(CH_3NH_3)_{n-1}Pb_nI_{3n+1}$(m=4–9; n=1–4). *J. Am. Chem. Soc.* **2018**, *140*, 12226–12238. [CrossRef] [PubMed]
165. Stoumpos, C.C.; Cao, D.H.; Clark, D.J.; Young, J.; Rondinelli, J.M.; Jang, J.I.; Hupp, J.T.; Kanatzidis, M.G. Ruddlesden-Popper Hybrid Lead Iodide Perovskite 2D Homologous Semiconductors. *Chem. Mater.* **2016**, *28*, 2852–2867. [CrossRef]

166. Battle, P.D.; Green, M.A.; Lago, J.; Millburn, J.E.; Rosseinsky, M.J.; Vente, J.F. Crystal and Magnetic Structure of $Ca_4Mn_3O_{10}$, an n=3 Ruddlesden-Popper compound. *Chem. Mater.* **1998**, *10*, 658–664. [CrossRef]
167. Dion, M.; Ganne, M.; Tournoux, M. Nouvelles familles de phases $MIMII_2Nb_3O_{10}$ a feuillets "Perovskites". *Mater. Res. Bull.* **1981**, *16*, 1429–1435. [CrossRef]
168. Hojamberdiev, M.; Bekheet, M.F.; Zahedi, E.; Wagata, H.; Kamei, Y.; Yubuta, K.; Gurlo, A.; Matsushita, N.; Domen, K.; Teshima, K.; et al. New Dion-Jacobson Phase Three-Layer Perovskite $CsBa_2Ta_3O_{10}$ and Its Conversion to Nitrided Ba2Ta3O10 Nanosheets via a Nitridation-Protonation-Intercalation-Exfoliation Route for Water Splitting. *Cryst. Growth Des.* **2016**, *16*, 2302–2308. [CrossRef]
169. Mao, L.; Ke, W.; Pedesseau, L.; Wu, Y.; Katan, C.; Even, J.; Wasielewski, M.R.; Stoumpos, C.C.; Kanatzidis, M. Hybrid Dion-Jacobson 2D Lead Iodide Structures. *J. Am. Chem. Soc.* **2018**, *140*, 3775–3783. [CrossRef] [PubMed]
170. Cao, D.H.; Stoumpos, C.C.; Farha, O.K.; Hupp, J.T.; Kanatzidis, M.G. 2D Homologous Perovskites as Light-Absorbing Materials for Solar Cell Applications. *J. Am. Chem. Soc.* **2015**, *137*, 7843–7850. [CrossRef]
171. Kagan, C.R.; Mitzi, D.B.; Dimitrakopoulos, C.D. Organic-Inorganic Hybrid Materials as Semiconducting Channels in Thin-Film Field-Effect Transitions. *Science* **1999**, *286*, 945–947. [CrossRef]
172. Smith, I.C.; Hoke, E.T.; Solis-Ibarra, D.; McGehee, M.D.; Karunadasa, H.I. A Layered Hybrid Perovskite Solar-Cell Absorber with Enhanced Moisture Stability. Angew. *Chem. Int. Ed.* **2014**, *53*, 11232–11235. [CrossRef] [PubMed]
173. Tsai, H.; Nie, W.; Blancon, J.C.; Stoumpos, C.C.; Asadpour, R.; Harutyunyan, B.; Neukirch, A.J.; Verduzco, R.; Crochet, J.J.; Tretiak, S.; et al. High-efficiency two-dimensional Ruddlesden-Popper Perovskite Solar Cells. *Nature* **2016**, *536*, 312–316. [CrossRef]
174. Vos, A.D. Detailed balance limit of the efficiency of tandem solar cells. *J. Phys. D: Appl. Phys.* **1980**, *13*, 839–846. [CrossRef]
175. Ghosh, A. Possibilities and Challenges for the Inclusion of the Electric Vehicle (EV) to Reduce the Carbon Footprint in the Transport Sector: A Review. *Energies* **2020**, *13*, 2602. [CrossRef]
176. Ghosh, A.; Norton, B. Optimization of PV powered SPD switchable glazing to minimise probability of loss of power supply. Renew. *Energy* **2019**, *131*, 993–1001. [CrossRef]
177. Wu, G.; Liang, R.; Ge, M.; Sun, G.; Zhang, Y.; Xing, G. Surface Passivation Using 2D Perovskites toward Efficient and Stable Perovskite Solar Cells. *Adv. Mater.* **2022**, *34*, 2105635. [CrossRef] [PubMed]
178. Hoex, B. Functional Thin Films for High-Efficiency Solar Cells. PhD Thesis, Technische Universiteit Eindhoven, Eindhoven, The Netherlands, 2008.
179. Nundy, S.; Ghosh, A.; Mesloub, A.; Noaime, E.; Touahmia, M. Comfort Analysis of Hafnium (Hf) Doped ZnO Coated Self-Cleaning Glazing for Energy-Efficient. *Materials* **2022**, *15*, 4934. [CrossRef]
180. Nundy, S.; Ghosh, A. Thermal and visual comfort analysis of adaptive vacuum integrated switchable suspended particle device window for temperate climate. *Renew. Energy* **2020**, *156*, 1361–1372. [CrossRef]
181. Nundy, S.; Mesloub, A.; Alsolami, B.M.; Ghosh, A. Electrically actuated visible and near-infrared regulating switchable smart window for energy positive building: A review. *J. Clean. Prod.* **2021**, *301*, 126854. [CrossRef]
182. Nundy, S.; Ghosh, A.; Tahir, A.; Mallick, T.K. Role of Hafnium Doping on Wetting Transition Tuning the Wettability Properties of ZnO and Doped Thin Films: Self-Cleaning Coating for Solar Application. *ACS Appl. Mater. Interfaces* **2021**, *13*, 25540–25552. [CrossRef] [PubMed]
183. Nundy, S.; Ghosh, A.; Mallick, T.K. Hydrophilic and Superhydrophilic Self-Cleaning Coatings by Morphologically Varying ZnO Microstructures for Photovoltaic and Glazing Applications. *ACS Omega* **2020**, *5*, 1033–1039. [CrossRef] [PubMed]
184. Selvaraj, P.; Ghosh, A.; Mallick, T.K.; Sundaram, S. Investigation of semi-transparent dye-sensitized solar cells for fenestration integration. *Renew. Energy* **2019**, *141*, 516–525. [CrossRef]
185. Ghosh, A.; Selvaraj, P.; Sundaram, S.; Mallick, T.K. The colour rendering index and correlated colour temperature of dye-sensitized solar cell for adaptive glazing application. *Sol. Energy* **2018**, *163*, 537–544. [CrossRef]
186. Ghosh, A.; Sundaram, S.; Mallick, T.K. Colour properties and glazing factors evaluation of multicrystalline based semi-transparent Photovoltaic-vacuum glazing for BIPV application. *Renew. Energy* **2019**, *131*, 730–736. [CrossRef]
187. Ghosh, A.; Sarmah, N.; Sundaram, S.; Mallick, T.K. Numerical studies of thermal comfort for semi-transparent building integrated photovoltaic (BIPV) -vacuum glazing system. *Sol. Energy* **2019**, *190*, 608–616. [CrossRef]
188. Ghosh, A.; Sundaram, S.; Mallick, T.K. Investigation of thermal and electrical performances of a combined semi-transparent PV-vacuum glazing. *Appl. Energy* **2018**, *228*, 1591–1600. [CrossRef]
189. Alrashidi, H.; Ghosh, A.; Issa, W.; Sellami, N.; Mallick, T.K.; Sundaram, S. Thermal performance of semitransparent CdTe BIPV window at temperate climate. *Sol. Energy* **2020**, *195*, 536–543. [CrossRef]
190. Alrashidi, H.; Ghosh, A.; Issa, W.; Sellami, N.; Mallick, T.K.; Sundaram, S. Evaluation of solar factor using spectral analysis for CdTe photovoltaic glazing. *Mater. Lett.* **2019**, *237*, 332–335. [CrossRef]
191. Alrashidi, H.; Issa, W.; Sellami, N.; Ghosh, A.; Mallick, T.K.; Sundaram, S. Performance assessment of cadmium telluride-based semi-transparent glazing for power saving in façade buildings. *Energy Build.* **2020**, *215*, 109585. [CrossRef]
192. Ghosh, A.; Mesloub, A.; Touahmia, M.; Ajmi, M. Visual Comfort Analysis of Semi-Transparent Perovskite Based Building Integrated Photovoltaic Window for Hot Desert. *Energies* **2021**, *14*, 1043. [CrossRef]
193. Ghosh, A.; Bhandari, S.; Sundaram, S.; Mallick, T.K. Carbon counter electrode mesoscopic ambient processed & characterised perovskite for adaptive BIPV fenestration. *Renew. Energy* **2020**, *145*, 2151–2158. [CrossRef]
194. Roy, A.; Ullah, H.; Ghosh, A.; Baig, H.; Sundaram, S.; Tahir, A.A.; Mallick, T.K. Understanding the Semi-Switchable Thermochromic Behavior of Mixed Halide Hybrid Perovskite Nanorods. *J. Phys. Chem. C* **2021**, *125*, 18058–18070. [CrossRef]

195. Bhandari, S.; Ghosh, A.; Roy, A.; Kumar, T.; Sundaram, S. Compelling temperature behaviour of carbon-perovskite solar cell for fenestration at various climates. *Chem. Eng. J. Adv.* **2022**, *10*, 100267. [CrossRef]
196. Shaik, S.; Nundy, S.; Ramana, V.; Ghosh, A.; Afzal, A. Polymer dispersed liquid crystal retrofitted smart switchable glazing: Energy saving, diurnal illumination, and CO_2 mitigation prospective. *J. Clean. Prod.* **2022**, *350*, 131444. [CrossRef]
197. Mesloub, A.; Ghosh, A.; Touahmia, M.; Abdullah, G.; Alsolami, B.M.; Ahriz, A. Assessment of the overall energy performance of an SPD smart window in a hot desert climate The International Commission on Illumination. *Energy* **2022**, *252*, 124073. [CrossRef]
198. Chidubem Iluyemi, D.; Nundy, S.; Shaik, S.; Tahir, A.; Ghosh, A. Building energy analysis using EC and PDLC based smart switchable window in Oman. *Sol. Energy* **2022**, *237*, 301–312. [CrossRef]
199. Ghosh, A.; Norton, B.; Duffy, A. Measured overall heat transfer coefficient of a suspended particle device switchable glazing. *Appl. Energy* **2015**, *159*, 362–369. [CrossRef]
200. Ghosh, A.; Norton, B.; Duffy, A. Behaviour of a SPD switchable glazing in an outdoor test cell with heat removal under varying weather conditions. *Appl. Energy* **2016**, *180*, 695–706. [CrossRef]
201. Ghosh, A.; Norton, B.; Duffy, A. Measured thermal performance of a combined suspended particle switchable device evacuated glazing. *Appl. Energy* **2016**, *169*, 469–480. [CrossRef]
202. Ghosh, A.; Norton, B.; Duffy, A. Measured thermal & daylight performance of an evacuated glazing using an outdoor test cell. *Appl. Energy* **2016**, *177*, 196–203. [CrossRef]
203. Ghosh, A.; Norton, B.; Duffy, A. First outdoor characterisation of a PV powered suspended particle device switchable glazing. *Sol. Energy Mater. Sol. Cells* **2016**, *157*, 1–9. [CrossRef]
204. Ghosh, A.; Norton, B.; Duffy, A. Effect of sky clearness index on transmission of evacuated (vacuum) glazing. *Renew. Energy* **2017**, *105*, 160–166. [CrossRef]
205. Ghosh, A.; Norton, B.; Duffy, A. Effect of sky conditions on light transmission through a suspended particle device switchable glazing. *Sol. Energy Mater. Sol. Cells* **2017**, *160*, 134–140. [CrossRef]
206. Ghosh, A.; Norton, B.; Duffy, A. Effect of atmospheric transmittance on performance of adaptive SPD-vacuum switchable glazing. *Sol. Energy Mater. Sol. Cells* **2017**, *161*, 424–431. [CrossRef]
207. Ghosh, A.; Norton, B. Durability of switching behaviour after outdoor exposure for a suspended particle device switchable glazing. *Sol. Energy Mater. Sol. Cells* **2017**, *163*, 178–184. [CrossRef]
208. Ghosh, A.; Norton, B. Interior colour rendering of daylight transmitted through a suspended particle device switchable glazing. *Sol. Energy Mater. Sol. Cells* **2017**, *163*, 218–223. [CrossRef]